Accepted Manuscript

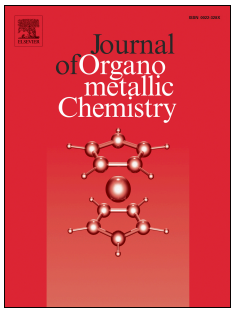

Synthesis and properties of Fischer carbene complexes of *N,N*-dimethylaniline and anisole π-coordinated to chromium tricarbonyl

Nora-ann Weststrate, Shalane Bouwer, Christopher Hassenrück, Nina A. van Jaarsveld, David C. Liles, Rainer F. Winter, Simon Lotz

PII: S0022-328X(18)30397-8

DOI: 10.1016/j.jorganchem.2018.05.022

Reference: JOM 20456

To appear in: *Journal of Organometallic Chemistry*

Received Date: 24 May 2018

Accepted Date: 25 May 2018

Please cite this article as: N.-a. Weststrate, S. Bouwer, C. Hassenrück, N.A. van Jaarsveld, D.C. Liles, R.F. Winter, S. Lotz, Synthesis and properties of Fischer carbene complexes of *N,N*-dimethylaniline and anisole π-coordinated to chromium tricarbonyl, *Journal of Organometallic Chemistry* (2018), doi: 10.1016/j.jorganchem.2018.05.022.

This is a PDF file of an unedited manuscript that has been accepted for publication. As a service to our customers we are providing this early version of the manuscript. The manuscript will undergo copyediting, typesetting, and review of the resulting proof before it is published in its final form. Please note that during the production process errors may be discovered which could affect the content, and all legal disclaimers that apply to the journal pertain.

ACCEPTED MANUSCRIPT

Synthesis and properties of Fischer carbene complexes of *N*,*N*-dimethylaniline and anisole π-coordinated to chromium tricarbonyl

Nora-ann Weststrate[a], *Shalane Bouwer*[a], *Christopher Hassenrück*[b], *Nina A. van Jaarsveld*[a], *David C. Liles*[a], *Rainer F. Winter*[b]* *and Simon Lotz*[a]*

[a]Department of Chemistry, University of Pretoria, Pretoria, 0002, South Africa

[b]Fachbereich Chemie, Universität Konstanz, Konstanz, 78457, Germany

KEYWORDS

Fischer carbene complexes; heterobi- and –trimetallic complexes; X-ray crystallography; (spectro)electrochemistry; quantum chemical calculations.

ABSTRACT

The reaction of lithiated N,N-dimethylaniline π-coordinated to $Cr(CO)_3$ with $W(CO)_6$ and alkylation with $[Et_3O][BF_4]$ afforded the *o*-, *m*- and *p*-isomers of the σ,π-bimetallic complexes $\{\eta^6\text{-}Me_2NC_6H_4C(OEt)W(CO)_5\}Cr(CO)_3$ (*o*-, **1**, *m*-, **2** and *p*-isomer, **3**). A by-product of the reaction is found by the substitution of a carbonyl ligand in **1** by the aniline nitrogen atom to give $\{\eta^6\text{-C,N-}o\text{-}Me_2NC_6H_4C(OEt)W(CO)_4\}Cr(CO)_3$ (**4**). As a result, the W-chelate ring dominates

the HOMO rather than the{η^6-areneCr$(CO)_3$} fragment, affecting the site of the first oxidation. Enhanced activation of anisole by π-coordination to $Cr(CO)_3$, and subsequent reactions with *n*BuLi, $W(CO)_6$ and $[Et_3O][BF_4]$ gave only *o*-substituted products {$\mu,\eta^{6:1}$-*o*-$MeOC_6H_4C(OEt)W(CO)_5$}$Cr(CO)_3$ (**5**), the monocarbene chelate {$\mu,\eta^{6:2}$-C,O-*o*-$MeOC_6H_4C(OEt)W(CO)_4$}$Cr(CO)_3$ (**6**) by carbonyl substitution, and by reaction of two molar equivalents reagents, the unique σ,σ,π-heterotrimetallic biscarbene complex {$\mu_3,\eta^{6:1:1}$-*o*,*o*-$MeOC_6H_3(C(OEt)W(CO)_5)_2$}$Cr(CO)_3$ (**7**). Attempts to synthesise the *m*- and *p*-isomers of **5** were unsuccesful due to transmetallation of the lithiated precursors. NMR data confirmed that lithiation and subsequent reactions of *m*- or *p*-bromoanisol chromiumtricarbonyl afforded only the *o*-isomer **5** and {η^6-$MeOC_6H_5$}$Cr(CO)_3$. Crystal structure determinations of complexes **1**-**7** confirmed their molecular structures. Spectroscopic data, electrochemistry studies and DFT calculations of the complexes are reported and in line with a shifting of the HOMO from the $Cr(CO)_3$ to the $W(CO)_4$ chelate entities and with an unusually large delocalisation of the HOMO of the other complexes onto the π-coordinated arene ligand and the carbene-bonded metal atom.

1. Introduction

Activation of specific sites on aryl rings has been a synthetic challenge relevant to the fields of medicinal and organic chemistry for many years.[1,2] Relying on directing substituents can partially solve this problem, but poor reactivity of such donor-substituted arenes often limits the efficiency of this strategy. Coordination of benzene derivatives to a chromium tricarbonyl fragment changes the electronic properties of the arene ring and influences the chemical reactivity and selectivity of subsequent substitution reactions. For monosubstituted benzenes π-coordinated to $Cr(CO)_3$, the ordering F >> OMe > NMe_2 with respect to their ability to direct

lithiation to the *o*-position has been established.[3] However, a better understanding of the regioselective activation of substituted aryl rings π-coordinated to $Cr(CO)_3$, and in particular the intricate interplay between electronic and steric effects, remains elusive and warrants further investigation.

The combination of two transition metals in σ,π-coordinated homo- and heterobimetallic complexes with benzene linkers greatly expands the scope of their applications in organic synthesis.[4] The rate of insertion of palladium into carbon-halogen bonds of phenyl halides, for example, is enhanced by their π-coordination to $Cr(CO)_3$, owing to the strong electron withdrawing properties of the $Cr(CO)_3$ fragment. This aspect has been widely exploited in carbon-carbon coupling reactions.[5,6] In the synthesis of σ,π-coordinated bimetallic complexes derived from (η^6-arene)$Cr(CO)_3$ precursors with ring-substituted benzene rings, the positioning of the σ-bonded transition metal fragments is controlled by the directing effect as well as the electronic and steric properties of the ring substituents and the π-coordinated $Cr(CO)_3$ unit.[7–9]

Only few examples of σ,π-bimetallic complexes where the σ-metal substituent is a Fischer transition metal carbene complex have been documented in literature.[10–12] This is presumably so because both the Fischer carbene moiety $(CO)_5M\{C(OR)R'\}$ and the $Cr(CO)_3$ entity represent electron-withdrawing fragments that compete for π-electron density from a σ,π-bridging benzene linker.[13–16] The aims of the present study are (i) to find effective methods of synthesis for the different isomers of σ,π-bimetallic complexes of *N*,*N*-dimethylaniline and anisole π-coordinated to $Cr(CO)_3$ with attached $(CO)_5W\{C(OEt)\}$-substituents and (ii) to study and further our understanding of the electronic and structural features of this rare class of σ,π-bimetallic carbene complexes. The two precursors differ in that the dimethylamino substituent represents the superior electron donor while the methoxy substituent has the greater *o*-directing capability.

2. Experimental

2.1 General: Syntheses of the complexes were conducted in an atmosphere of nitrogen or argon using standard Schlenk techniques. Column chromatography, using Silica gel 60 (particle size 0.0063 – 0.200 mm), was used for all separations. CH_2Cl_2 was distilled over CaH_2 while THF and hexane were distilled over sodium metal. All other reagents were used as received from commercial suppliers. NMR spectra were recorded in $CDCl_3$ as solvent on a Bruker Ultrashield 300 AVANCE 3 or a Bruker Ultrashield Plus 400 AVANCE 3 spectrometer at 298 K. The NMR spectra were recorded for ^1H at 300.13 or 400.13 MHz while the ^{13}C spectra were recorded at 75.468 or 100.163 MHz. Chemical shifts are reported in ppm, using the deuterated solvent signal as the internal reference ($CDCl_3$: δ ^1H = 7.26, δ ^{13}C at 77.16 ppm). Infrared (IR) spectroscopy in the carbonyl region was recorded on a Bruker ALPHA FT-IR spectrophotometer in a NaCl cell using hexane as solvent. Single X-ray crystallographic data were obtained at T = 20° C on a Siemens P4 diffractometer fitted with a Bruker 1 K CCD detector using graphite monochromated Mo−Kα radiation by means of a combination of phi and omega scans. Cyclic voltammetry was performed in a one-compartment cell with Pt and Ag wires as counter and reference electrodes, respectively, while a Pt electrode (1.6 cm diameter from BAS) was used as a working electrode and CH_2Cl_2 as the solvent. Before measurements, the working electrode was polished with 1 µm and 0.25 µm diamond pastes (Buehler-Wirtz). NBu_4PF_6 (0.1 mM) was used as the supporting electrolyte. Referencing was done with the aid of an internal standard (ferrocene (Cp_2Fe) or decamethylferrocene (Cp^*_2Fc), which was added to the sample solution after all data was acquired. Representative sets of scans were repeated in the presence of the internal standard. Final referencing was done against the $Cp_2Fe^{0/+}$ couple with $E_{½}$ ($Cp^*_2Fc^{0/+}$) = -540 mV *vs.*

$Cp_2Fe^{0/+}$ in the used electrolyte. Spectroelectrochemistry (SEC) data were acquired with a computer-controlled BAS potentiostat. A home-built optically transparent thin layer electrolysis cell equipped with CaF_2 windows, Pt mesh as the working and counter electrodes, and thin silver sheet as the pseudo-reference electrode following the design of Hartl and coworkers was used.[17] FT-IR spectra were recorded on a Thermo is10 instrument. UV-Vis/NIR spectra were obtained on a TIDAS fiber optic diode array spectrometer (combined MCS UV/NIR and PGS NIR instrumentation) from j&m. Density functional theory (DFT) calculations were performed on the full model complexes using the Turbomole 7.1 program package.[18] Geometry optimizations were performed without any symmetry constraints. Within Turbomole calculations the valence polarised triple-ζ basis sets (def2-TZVP)[19–21] were employed for all atoms together with the b3-lyp[22,23] (complexes **1** to **4**) or pbe1pbe functional (complexes **5** to **7**).[24] Solvation effects were modelled by COSMO during the optimization process.[25]

2.2 Synthesis. $\{\eta^6\text{-}Me_2NC_6H_5\}Cr(CO)_3$ and **$\{\eta^6\text{-}MeOC_6H_5\}Cr(CO)_3$** were synthesised according to published methods by Mahaffy and co-workers.[26]

2.3 Synthesis of 1 and 4: 1.29 g of $\{\eta^6\text{-}Me_2NC_6H_5\}Cr(CO)_3$ (5.00 mmol) was dissolved in 10 mL of THF and lithiated with 3.13 mL of *n*BuLi (1.6 M) at –40 °C. After stirring at ambient temperature for 60 minutes, the reaction mixture was cooled to –40 °C and 1.76 g of $W(CO)_6$ (5.00 mmol) was added. The reaction mixture was allowed to stir at ambient temperature until all metal carbonyl had dissolved (approximately 60 minutes). The solvent was evaporated, and the reaction mixture was dissolved in CH_2Cl_2, cooled to –40 °C, and 0.95 g of $[Et_3O][BF_4]$ (5.00 mmol) were added. After the reaction mixture reached ambient temperature, it was passed through a silica plug using CH_2Cl_2 as solvent and the solvent was evaporated. The products were

isolated by chromatography on a silica gel column using hexane and CH_2Cl_2 as solvents. Yield: **1** = 2.13 g (66.9 %), **4** = 0.283 g (9.3 %).

2.4 Synthesis of 2 and 3: 1.29 g of $\{\eta^6\text{-}Me_2NC_6H_5\}Cr(CO)_3$ (5.00 mmol) were dissolved in 10 mL of THF and lithiated with 3.13 mL of *n*BuLi (1.6 M) at –40 °C, after which it was allowed to stir in the cold bath for 15 minutes. 1.76 g of $W(CO)_6$ (5.00 mmol) were added to the reaction mixture. It was allowed to stir in the cold bath for 30 minutes and then at RT until all metal carbonyl had dissolved (60 minutes). The solvent was removed *in vacuo*, and the reaction mixture was dissolved in 20 mL of CH_2Cl_2 and cooled to –40 °C. 0.95 g of $[Et_3O][BF_4]$ (5.00 mmol) were dissolved in 10 mL of CH_2Cl_2 and added to the cold solution while stirring. After allowing the reaction mixture to reach ambient temperature, it was passed through a silica plug. The products were isolated using a silica gel column and hexane and CH_2Cl_2 (12:1) as solvents. Yield: **2** = 1.68 g (52.7 %), **3** = 0.549 g (17.2 %).

2.5 Synthesis of 5, 6 and 7: 1.22 g of $\{\eta^6\text{-}MeOC_6H_5\}Cr(CO)_3$ (5.00 mmol) were dissolved in 10 mL of THF. The reaction mixture was lithiated at –40 °C with 3.31 mL *n*BuLi (1.6 M) and allowed to stir at ambient temperature for 60 minutes. 1.76 g of $W(CO)_6$ (5.00 mmol) was added to the reaction mixture at –40 °C. The reaction mixture was stirred at ambient temperature until all metal carbonyl had dissolved (60 minutes). The solvent was evaporated, and the reaction mixture was dissolved in CH_2Cl_2 and cooled to –40 °C. 0.95 g of $[Et_3O][BF_4]$ (5.00 mmol), dissolved in CH_2Cl_2, were added to the cold solution. After allowing the reaction mixture to reach ambient temperature, it was passed through a silica plug. The products were isolated using a silica gel column with hexane and CH_2Cl_2 as solvents (12:1). Yield: **5** = 1.44 g (46.1 %), **6** = 0.190 g (6.37 %), **7** = 0.882 g (23.8 %).

2.6 Characterisation: The π-coordination of *m*- and *p*-bromoanisole to $Cr(CO)_3$ and subsequent reaction with *t*BuLi, $W(CO)_6$ and $[Et_3O][BF_4]$ were followed by NMR spectroscopy and are described in the Supporting Information (SI).[27]

Assignment of the NMR resonance signals (^1H and ^{13}C) follows the atomic numbering provided in Figure 1. NMR spectra of all complexes can be found as Figures S-1 to S-16 of the Supporting Information (SI).

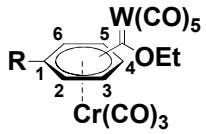

complexes **1 - 4:** R = NMe_2
complexes **5 - 7:** R = OMe

Figure 1. NMR assignments of **1-7**

1: $C_{19}H_{15}O_9NCrW$. ^1H NMR ($CDCl_3$, 300 MHz) δ 5.54 (ddd, *J* = 6.4, 6.1, 1.4 Hz, 1H, H5), 5.31 (d, *J* = 6.9 Hz, 1H, H3), 5.04 (q, *J* = 7.1 Hz, 2H, CH_2(OEt)), 4.96 (dd, *J* = 6.4, 1.4 Hz, 1H, H6), 4.89 (dd, *J* = 6.9, 6.1 Hz, 1H, H4), 2.71 (s, 6H, NMe_2), 1.78 (t, *J* = 7.1 Hz, 3H, CH_3 (OEt)). ^{13}C NMR ($CDCl_3$, 75 MHz) δ 320.4 (J_{WC} = 54.5 Hz, C_{carb}), 234.0 ($Cr(CO)_3$), 203.5 (J_{WC} = 56.0 Hz, $W(CO)_5$, *trans*) 196.6 (J_{WC} = 63.3 Hz, $W(CO)_5$, *cis*), 125.8 (C2), 114.9 (C1), 94.6 (C5), 91.6 (C6), 83.1 (C3), 82.2 (C4), 81.2 (CH_2(OEt)), 43.9 (NMe_2), 14.5 (CH_3(OEt)). TOF-MS. Calcd for $C_{18}H_{16}O_8NCrW$ ($[M–CO]^-$): *m/z* 609.9746. Found: *m/z* 609.9741.

2: $C_{19}H_{15}O_9NCrW$. ^1H NMR ($CDCl_3$, 300 MHz) δ 5.57 (dd, *J* = 7.0, 6.6 Hz, 1H, H5), 5.53 (s, 1H, H2), 5.48 (d, *J* = 6.6 Hz, 1H, H4), 5.08 (dq, *J* = 7.0, 2.3 Hz, 2H, CH_2(OEt)), 5.05 (d, *J* = 7.0 Hz, 1H, H6), 2.97 (s, 6H, NMe_2), 1.70 (t, *J* = 7.1 Hz, 3H, CH_3(OEt)). ^{13}C NMR ($CDCl_3$, 75 MHz) δ 311.0 (J_{WC} = 53.7 Hz, C_{Carb}), 234.4 ($Cr(CO)_3$), 202.4 (J_{WC} = 58.4 Hz, $W(CO)_5$, *trans*), 197.0 (J_{WC} = 63.5 Hz, $W(CO)_5$, *cis*), 133.1 (C3), 115.1 (C1), 94.3 (C5), 86.3 (C4), 80.2

(CH_2(OEt)), 78.9 (C2), 75.5 (C5), 40.0 (NMe_2), 14.9 (CH_3(OEt)). TOF-MS. Calcd for $C_{19}H_{16}O_9NCrW$ ($[M+H]^+$): *m/z* 637.9739. Found: *m/z* 637.9786.

3: $C_{19}H_{15}O_9NCrW$. ^{1}H NMR ($CDCl_3$, 300 MHz) δ 6.34 (d, *J* = 7.7 Hz, 2H, H3 and H5), 4.93 (q, *J* = 7.1 Hz, 2H, CH_2(OEt)), 4.87 (d, *J* = 7.7 Hz, 2H, H2 and H6), 3.01 (s, 6H, NMe_2), 1.65 (t, *J* = 7.0 Hz, 3H, CH_3(OEt)). ^{13}C NMR ($CDCl_3$, 75 MHz) δ 302.9 (J_{WC} = n.o., C_{Carb}), 231.9 ($Cr(CO)_3$), 202.1 (J_{WC} = n.o., $W(CO)_5$, *trans*) 197.3 (J_{WC} = 63.1 Hz, $W(CO)_5$, *cis*), 136.8 (C4), 105.6 (C1), 99.5 (C3 and C5), 79.2 (CH_2(OEt)), 73.1 (C2 and C6), 40.0 (NMe_2), 15.1 (CH_3(OEt)). TOF-MS. Calcd for $C_{19}H_{16}O_9NCrW$ ($[M–H]^-$): *m/z* 637.9774. Found: *m/z* 637.9769.

4: $C_{18}H_{15}O_8NCrW$. ^{1}H NMR ($CDCl_3$, 300 MHz) δ 5.85 (dd, *J* = 6.6, 0.9 Hz, 1H, H3), 5.72 (d, *J* = 6.5 Hz, 1H, H6), 5.54 (ddd, *J* = 7.1, 6.6, 0.9 Hz, 1H, H4), 5.34 (dd, *J* = 7.1, 6.5 Hz, 1H, H5), 5.04 – 4.89 (m, 2H, CH_2(OEt)), 3.66 (s, 3H, NMe), 3.45 (s, 3H, NMe), 1.70 (t, *J* = 7.1 Hz, 3H, CH_3(OEt)). ^{13}C NMR ($CDCl_3$, 75 MHz) δ 305.2 (J_{WC} = n.o., C_{Carb}), 230.7 ($Cr(CO)_3$), 222.2 (J_{WC} = n.o., $W(CO)_4$), 213.1 (J_{WC} = n.o., $W(CO)_4$), 205.8 (J_{WC} = n.o., $W(CO)_4$), 203.7 (J_{WC} = n.o., $W(CO)_4$), 137.5 (C2), 110.4 (C3), 91.4 (C5), 90.5 (C1), 84.5 (C6), 83.3 (C4), 79.5 (CH_2(OEt)), 64.4 (NMe), 57.5 (NMe), 15.2 (CH_3(OEt)). TOF-MS. Calcd for $C_{18}H_{16}O_8NCrW$ ($[M–H]^-$): *m/z* 609.9790. Found: *m/z* 609.9760.

5: $C_{18}H_{12}O_{10}CrW$. ^{1}H NMR ($CDCl_3$, 400 MHz) δ 5.60 (ddd, *J* = 6.7, 6.2, 1.3 Hz, 1H, H5), 5.29 (dd, *J* = 6.2, 1.3 Hz, 1H, H3), 5.01 (dd, *J* = 6.2, 0.5 Hz, 1H, H6), 4.98 (dq, *J* = 7.1, 1.1 Hz, 2H, CH_2(OEt)), 4.81 (ddd, *J* = 6.7, 6.2, 0.8 Hz, 1H, H4), 3.72 (s, 3H, CH_3(OMe)), 1.76 (t, *J* = 7.1 Hz, 3H, CH_3(OEt)). ^{13}C NMR ($CDCl_3$, 101 MHz) δ 315.7 (J_{WC} = n.o., C_{Carb}), 232.6 ($Cr(CO)_3$), 203.9 (J_{WC} = n.o., $W(CO)_5$, *trans*), 196.6 (J_{WC} = 64.0 Hz, $W(CO)_5$, *cis*), 136.6 (C1), 117.8 (C2), 94.6 (C5), 91.0 (C3), 81.6 (C4), 81.0 (CH_2(OEt)), 71.7 (C6), 55.8 (CH_3(OMe)), 14.5 (CH_3(OEt)). TOF-MS. Calcd for $C_{18}H_{13}O_{10}CrW$ ($[M+H]^+$): *m/z* 623.9416. Found: *m/z* 623.9418.

6: $C_{17}H_{12}O_9CrW$. ^{1}H NMR ($CDCl_3$, 400 MHz) δ 6.27 (d, *J* = 6.3 Hz, 1H, H3), 5.78 (dd, *J* = 6.8, 6.2 Hz, 1H, H5), 5.38 (d, *J* = 6.2 Hz, 1H, H6), 5.01 (q, *J* = 7.2 Hz, 2H, CH_2(OEt)), 4.91 (dd, *J* = 6.8, 6.3 Hz, 1H, H4), 4.50 (s, 3H, CH_3(OMe)), 1.76 (t, *J* = 7.1 Hz, 3H, CH_3(OEt)). ^{13}C NMR ($CDCl_3$, 101 MHz) δ 304.1 (J_{WC} = n.o., C_{Carb}), 230.0 ($Cr(CO)_3$), 219.7 (J_{WC} = n.o., $W(CO)_4$), 217.2 (J_{WC} = n.o., $W(CO)_4$), 217.2 (J_{WC} = n.o., $W(CO)_4$), 214.2 (J_{WC} = n.o., $W(CO)_4$), 122.7 (C1), 114.7 (C2), 93.3 (C5), 88.4 (C3), 84.8 (CH_2(OEt)), 73.4 (C6), 73.4 (C4), 67.8 (CH_3(OMe)), 15.3 (CH_3(OEt)). TOF-MS. Calcd for $C_{17}H_{12}O_9CrW$ ($[M]^+$): *m/z* 595.9422. Found: *m/z* 595.9419.

7: $C_{26}H_{16}O_{16}CrW_2$. ^{1}H NMR ($CDCl_3$, 400 MHz) δ 5.17 (d, *J* = 6.2 Hz, 2H, H3), 5.11-4.93 (m, 4H, CH_2(OEt)), 5.00 (d, *J* = 6.3 Hz, 1H, H4), 3.63 (s, 3H, CH_3(OMe)), 1.76 (t, *J* = 7.1 Hz, 6H, CH_3(OEt)). ^{13}C NMR ($CDCl_3$, 101 MHz) δ 315.4 (J_{WC} = n.o., C_{Carb}), 232.3 ($Cr(CO)_3$), 203.5 (J_{WC} = n.o., $W(CO)_5$, *trans*), 196.2 (J_{WC} = 64.0 Hz, $W(CO)_5$, *cis*), 128.7 (C1), 119.6 (C2), 89.3 (C3), 81.2 (CH_2(OEt)), 81.1 (C4), 65.0 (CH_3(OMe)), 14.6 (CH_3(OEt)). TOF-MS. Calcd for $C_{26}H_{17}O_{16}CrW_2$ ($[M+H]^+$): *m/z* 1005.8947. Found: *m/z* 1005.8873.

3. Results and Discussion

3.1 Synthesis. High yields of $\{\eta^6\text{-}RC_6H_5\}Cr(CO)_3$ (R = NMe_2, OMe) were obtained by refluxing $Cr(CO)_6$ with excess *N*,*N*-dimethylaniline or anisole in a 10:1 mixture of dibutyl ether and THF overnight.[26] Coordination of *N*,*N*-dimethylaniline required half the time than that required for coordination of anisole presumably because of the increased electron density present on the aromatic ring of the *N*,*N*-dimethylaniline. The reaction of $\{\eta^6\text{-}Me_2NC_6H_5\}Cr(CO)_3$ or $\{\eta^6\text{-}MeOC_6H_5\}Cr(CO)_3$ with one molar equivalent of *n*BuLi in THF at low temperature and subsequent treatment of the reaction mixture with $W(CO)_6$ and $[Et_3O][BF_4]$ affords the neutral

σ,π-coordinated bimetallic carbene complexes **1**-**7** shown in Schemes 1 and 2. Due to activation of the arene ring by the $Cr(CO)_3$ group, all positional isomers of the heterobinuclear Cr, W complexes were obtained, albeit in different quantities and under different reaction conditions. Longer reaction times and higher reaction temperatures provide selectively the thermodynamically favoured *o*-ethoxycarbene complex {(μ,$\eta^{6:1}$-*o*-$Me_2NC_6H_4C(OEt)W(CO)_5$}$Cr(CO)_3$ (**1**) and the W-chelate complex {(μ,$\eta^{6:2}$- *C*,*N*-*o*-$Me_2NC_6H_4C(OEt)W(CO)_4$}$Cr(CO)_3$ (**4**), where the lone pair at the nitrogen atom of the *N*,*N*-dimethylaniline substituent has replaced a carbonyl ligand at tungsten. In contrast, conducting the same reaction at low temperatures (–40 °C) leads to the formation of the *meta* and *para* isomers of **1**, complexes **2** and **3**, as the kinetically favoured products (**Scheme 1**).

Scheme 1. Synthesis of σ,π-bimetallic carbene complexes of *N*,*N*-dimethylaniline, **1**-**4**

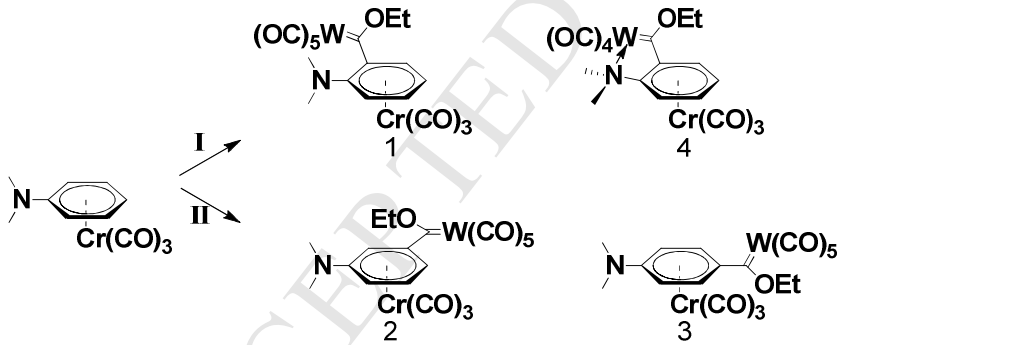

I. (Thermodynamic reaction)
i. *n*BuLi, -40°C, THF, stir 30 min
ii. 30°C, stir 60 min
iii. $W(CO)_6$, -40°C, THF, stir 30 min
iv. 30°C, stir 60 min
v. $[Et_3O][BF_4]$, -40°C, CH_2Cl_2

II. (Kinetic reaction)
i. *n*BuLi, -40°C, THF, stir 15 min
ii. $W(CO)_6$, -40°C, THF, stir 40 min
iii. $[Et_3O][BF_4]$, -40°C, CH_2Cl_2

The positional selectivity of substitution in {η^6-arene}$Cr(CO)_3$ complexes by a deprotonation/electrophilic addition sequence is often governed by contrasting kinetic and

thermodynamic site preferences and hence depends on the reaction conditions.[28] There is no indication that **2** or **3** are formed under thermodynamic control (conditions **I**), while trace amounts of **1** and **4** are observed under kinetic conditions, **II**. For **I**, the ratio between **1** and **4** is *ca* 70:30 while in **II**, **2** and **3** form in a ratio of 10:1. If less stringent reactions conditions are applied, all three positional isomers **1**-**3** can be obtained from a single experiment (*m* >> *p* > *o*). By contrast, reaction of uncomplexed *N*,*N*-dimethylaniline with *n*-butyllithium results mainly in *o*-lithiation.[29] π-Coordination of the benzene ring to $Cr(CO)_3$ increases the acidity of all protons on the ring markedly. Card and Trahanovsky have reported that lithiation of $\{\eta^6\text{-}NMe_2C_6H_5\}Cr(CO)_3$ and subsequent alkylation with MeI gives the *o*-, *m*-, and *p*-isomers of the methyl-*N*,*N*-dimethylaniline complex in a ratio of 30:52:18 % (*o*:*m*:*p*).[30] A ratio of 0:75:25 for these isomers has been found in the synthesis of the σ,π-bimetallic complexes $\{\mu,\eta^{6:1}\text{-}NMe_2C_6H_5(TiCp_2Cl)\}Cr(CO)_3$ in our laboratories after quenching with titanocene dichloride.[9] As the much larger bulkiness of the Cp_2TiCl and $C(OEt)W(CO)_5$ fragments compared to a methyl substituent is expected to dominantly affect the *o*-position, the above results can be deemed qualitatively in line with the results of Card and Trahanovsky. The presence of only trace amounts of the *o*-substituted carbene complexes **1** and **4** observed under kinetic conditions is thus also ascribed to steric constraints. The red complexes **1**-**3** and red-brown **4** were purified by column chromatography, recrystallised from dichloromethane/hexane and are all stable in the solid state.

Enhanced activation of anisole by π-coordination to $Cr(CO)_3$ and the strong Li^+ coordinating properties of the methoxy substituent clearly override the effect of unfavourable steric congestion. Therefore only *o*-carbene products were isolated (**Scheme 2**) in the reactions of the anisole complex with *n*BuLi, $W(CO)_6$ and $[Et_3O][BF_4]$. The major product is $\{\mu,\eta^{6:1}\text{-}o\text{-}$

$MeOC_6H_4C(OEt)W(CO)_5\}Cr(CO)_3$ (**5**), which slowly converts into the monocarbene tungsten tetracarbonyl chelate $\{\mu,\eta^{6:2}$-*C*,*O*-*o*-$MeOC_6H_4C(OEt)W(CO)_4\}Cr(CO)_3$ (**6**) by carbonyl substitution. Lithiated $\{\eta^6$-$OMeC_6H_5\}Cr(CO)_3$ likewise affords exclusively $\{\eta^6$-*o*-$OMeC_6H_4Me\}Cr(CO)_3$ after work-up with MeI [32] or $\{\mu,\eta^{6:1}$-*o*-$OMeC_6H_4(TiCp_2Cl)\}Cr(CO)_3$ after metallation with Cp_2TiCl_2.[31] The group of Ricci has recently shown that π-coordination of anisole to $Cr(CO)_3$ leads to selective *o*-arylation reactions, products that are otherwise unattainable.[32]

It has previously been reported that, as a result of the strong *o*-directing properties of the methoxy substituent in $\{\eta^6$-anisole$\}Cr(CO)_3$, the dilithiated intermediate can be formed in substantial amounts, even when an only slight excess of *n*BuLi is used.[30] Through the formation of this intermediate, the unique trinuclear biscarbene complex $\{\mu_3,\eta^{6:1:1}$-*o*,*o*-$MeOC_6H_3(C(OEt)W(CO)_5)_2\}Cr(CO)_3$) (**7**) is formed.[7]

Scheme 2. Synthesis of the heterobi- and -trimetallic carbene complexes **5**-**7** with π-coordinated anisole

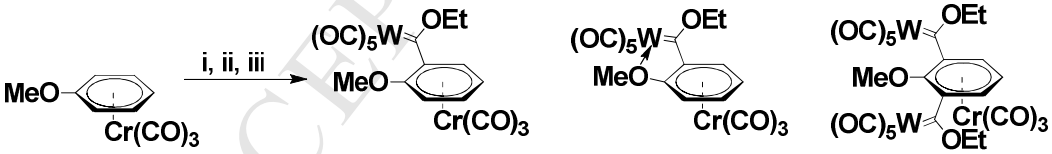

i. *n*BuLi, -40°C, THF
ii. $W(CO)_6$, -40°C, THF
iii. $[Et_3O][BF_4]$, -40°C, CH_2Cl_2

5 (46%) **6** (6.0%) **7** (23%)

The three products are red (**5**), red-brown (**6**), or purple (**7**) in colour and can be crystallised by layering concentrated solutions of the corresponding complexes in CH_2Cl_2 with hexane.

Although the amount of **6** that forms during a controlled reaction is relatively small, the product can be obtained in quantitative yield by UV irradiation of **5** in a hexane:THF 10:1 mixture. Similar homodimetallic complexes $\{\mu,\eta^{6:2}$-*C*,*X*-*o*-$RC_6H_4XC(OEt)Cr(CO)_4\}Cr(CO)_3$ of chromium containing carbene-methoxy and carbene-dimethylamino chelate rings have been reported for *o*-carbene complexes of anisole and *N*,*N*-dimethylaniline.[33,34] In these instances, the lone pair of the arene-bonded heteroatom substituent coordinates to $Cr(CO)_4$ or $W(CO)_4$ rather than participating in π-delocalization within the arene ring and stabilizing the electron-poor $Cr(CO)_3$ fragment.

It is noted here that the diversity of the σ,π-multinuclear complexes **1**-**7** is rare in the chemistry of carbene complexes.[7] Fischer and co-workers studied the synthesis of the different isomers of mononuclear $\{NMe_2C_6H_4C(OMe)Cr(CO)_5\}$ and $\{OMeC_6H_4C(OMe)Cr(CO)_5\}$ complexes. The reaction of *N*,*N*-dimethylaniline with *n*BuLi, followed by $Cr(CO)_6$ and alkylation with $[Me_3O][BF_4]$ did not afford the *o*-isomer and very little of the *m*- and *p*-isomers, presumably as a result of the quaternization of the nitrogen substituent (Figure 2).[35] The *o*-isomer was, however, prepared by the same method of synthesis several years later.[34] The *m*- and *p*-isomers of anisole tungsten carbene complexes could be prepared by lithium-bromine exchange reactions only, while the *o*-isomer was obtainable from deprotonation of the parent arene complex with *n*BuLi.[35]

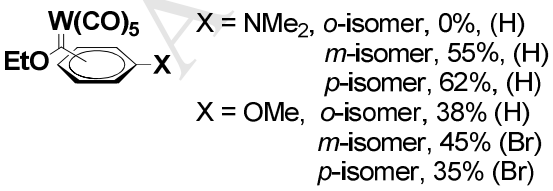

Figure 2. Fischer carbene complexes of dimethylaniline and anisole reported by Fischer [35]

All efforts to synthesise the *m*- or *p*-isomers of {μ,$\eta^{6:1}$-*o*-$OMeC_6H_4C(OEt)W(CO)_5$}$Cr(CO)_3$ (**5**) from the corresponding *m*- or *p*-substituted {η^6-bromoanisole}$Cr(CO)_3$ isomers were unsuccessful. The results are ascribed to enhanced activation of the anisole ring due to π-coordination to $Cr(CO)_3$ (see Scheme S-1 in the Supporting Information (SI)). Transmetallation (*halogen dancing*) from the *m*- or *p*- to the *o*-position is favoured and subsequent reactions with $W(CO)_6$ and $[Me_3O][BF_4]$ afford **5** as the only carbene isomer as a 1:1 mixture with (η^6-*o*-$OMeC_6H_5$}$Cr(CO)_3$ (**Scheme 3**).

Scheme 3. Attempted synthesis of {η^6-*m*-or *p*-$OMeC_6H_4C(OEt)W(CO)_5$}$Cr(CO)_3$

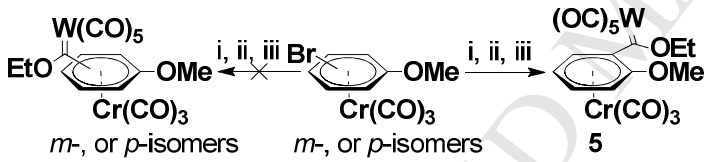

i. *n*BuLi, -40°C, THF
ii. $W(CO)_6$, -40°C, THF
iii. $[Et_3O][BF_4]$, -40°C, CH_2Cl_2

3.2 NMR Spectroscopy. The molecular structures of the new σ,π-heterobimetallic complexes in solution were verified by NMR and IR spectroscopy. Even though the heteroatom substituent of the arene ring (NMe_2 or OMe) plays an important role in determining the preferred deprotonation site, the differences between the chemical shifts in the ^{1}H NMR spectra of the remaining arene protons of **1** and **5** as well as **4** and **6** show only small differences. The most relevant observations in the ^{1}H NMR spectra are the large upfield shifts of more than 1 ppm of

all the ring protons because of π-coordination to the $Cr(CO)_3$ fragment. Interestingly, chemical shift of the amine methyl resonance does not correspond with the expectations of delocalization of the nitrogen lone pair into the arene π-system, as it shifts downfield from the *o*- to the *m*- and the *p*-isomer (2.71 (**1**) < 2.79 (**2**) < 3.01 (**3**) ppm). An inversed sequence with upfield shifts (320 (**1**) > 311 (**2**) > 303 (**3**) ppm) is observed for the carbene carbon atom in the ^{13}C NMR spectra. Clearly, resonance stabilization between the NMe_2 donor and the tungsten carbene acceptor does not play a role for **1** (Figure 3). Steric hindrance between the bulky neighbouring donor and acceptor substituents prevents their coplanar arrangement, as later confirmed by X-ray crystallography (*vide infra*). On this note, free rotation of the NMe_2 substituent is observed for all three isomers, such that only one methyl resonance signal is observed in their ^1H and ^{13}C NMR spectra. Due to the *p*-disposition of the electron donating NMe_2 and electron withdrawing tungsten carbonyl carbene fragment, **3** is symmetrically polarised. The protons α to these substituents in the arene ring differ strongly with respect to their chemical shifts of 4.87 and 6.34 ppm, respectively, which supports such a conclusion.

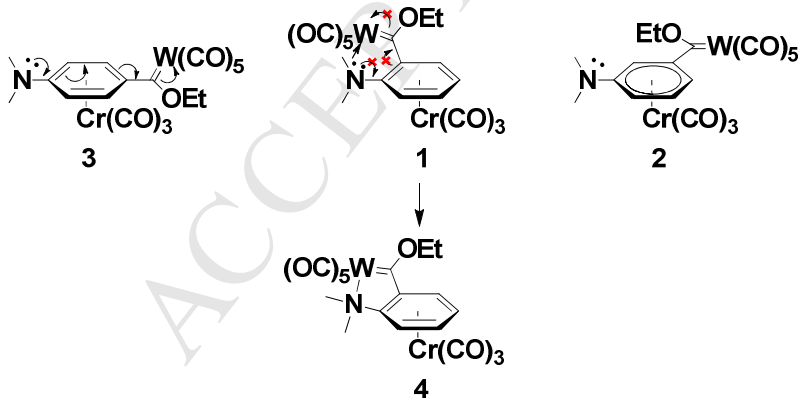

Figure 3. π-Resonance stabilization effects between the heteroatom and the carbene substituent in π-coordinated (arene)$Cr(CO)_3$ complexes of dimethylaniline

The arene protons and resonance signals of the heteroatom methyl groups are strongly shifted to lower field on coordination of the heteroatom lone-pair to the $W(CO)_4$ fragment. The *N*-methyl resonances shift from 2.71 (^{1}H) and 43.9 (^{13}C) in **1** to 3.66 and 3.45 ppm, or to 57.5 and 67.5 ppm for **4**. Note that the two methyl substituents of **4** are locked in different magnetic and electronic environments due to the formation of the chelate ring and their position (*syn* or *anti*) with respect to the $Cr(CO)_3$ tripod, resulting in two different resonances in the ^{13}C and ^{1}H NMR spectra. Similar large downfield shifts from 3.72 and 55.8 ppm to 4.50 and 67.8 ppm are noted for the pair of complexes **5** and **6**. Downfield proton shifts of *ca* 0.3 ppm on average for all ring protons indicate a transfer of electron density from the arene ligand to the chelate ring (Figure 4). The chemical shifts of the carbene carbon atom of complexes **4** (305.1 ppm) and **6** (304.1 ppm) are also upfield to those of **1** (320.4 ppm) and **5** (315.7 ppm), indicating more electron density on the carbene carbon atom due to chelation and the replacement of a CO ligand by the lone pair of the heteroatom substituent. The complexes with unsymmetrically substituted arene rings (all with the exception of **3** and **7**) display planar chirality which is manifested in a slight broadening of the resonance signals of the arene protons and multiple quartets for the methylene resonances of the ethoxycarbene substituents.[36,37]

ACCEPTED MANUSCRIPT

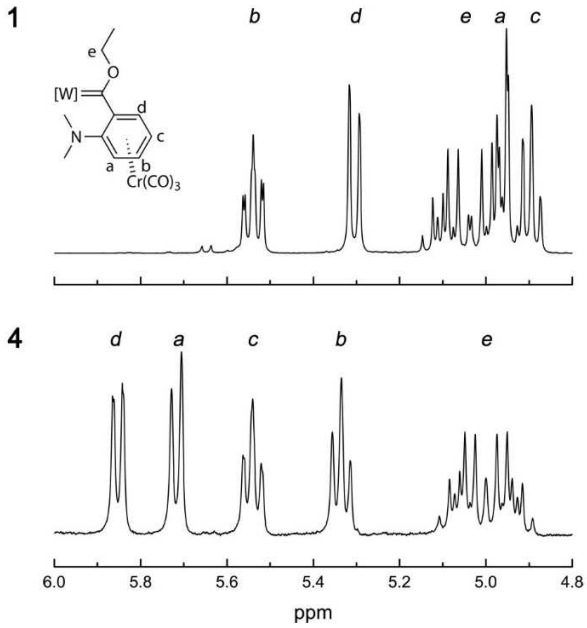

Figure 4. ^{1}H NMR spectra of the aromatic region of **1** (top) and **4** (bottom) in $CDCl_3$ at 298 K

3.3 IR Spectroscopy. The characteristic patterns and vibration frequencies of the bands in the carbonyl region of their infrared spectra confirm the presence of the corresponding metal-carbonyl entities $M(CO)_n$ (n = 3, 4 and 5) in the complexes.[38] Figure 5 shows the infrared spectra of complexes **2** and **4** in the carbonyl region as references while Table 1 provides a listing of the observed CO bands along with their assignment.

Table 1. Energies and assignments of the ν(CO) bands (in cm^{-1}) for complexes **1-7** in hexane at 298 K

$Cr(CO)_3$		$W(CO)_5$			
A_1	E	$A_1^{(1)}$	B_1	$A_1^{(2)}$	E

1	1982 (s), 1972	1906, 1896	2072	2004 (w)	1960 (m)	1952 (s), 1936 (s)
2	1972 (s)	1908 (br)	2068	1984 (w)	1954 (sh)	1944 (s)
3	1968 (s)	1896 (s), 1890 (s)	2068	1982 (w)	1948 (s)	1940 (br)
5	1983 (w)	1909 (w)	2079, 2073 (w)	1999 (w), 1991 (vw)	1955,1918 (w)	1969 (vs), 1934 (s)
7	1979 (s)	1912 (s)	2073	1989 (w)	1936 (s)	1961 (vs)
	$Cr(CO)_3$		$W(CO)_4$			
	A_1	E	$A_1^{(1)}$	$A_1^{(2)}$	B_1	B_2
4	1983 (vs)	1926 (s)	2027	1942	1916	1873
6	1983 (s), 1974 (w)	1908 (br)	2033 (w), 2025 (vw)	1940 (w), 1932 (w)	1919 (br)	1873 (br)

The two bands of a *fac*-$Cr(CO)_3$ entity, A_1 and E, are generally found at higher and lower wavenumbers, respectively, with respect to the $A_1^{(2)}$ and E bands of $W(CO)_5$. In the case of complexes **1**, **2**, **3** and **5**, the $A_1^{(2)}$ and E bands of the $W(CO)_5$ fragment overlap so that the $A_1^{(2)}$ band is observed as a shoulder of the E signal. For the aniline-derived complexes, this shoulder appears at the high-energy side, while it shows up at lower wavenumbers for the anisole complexes (Figures S-17 and S-18 of the SI).[39] Four bands ($A_1^{(1)}$, $A_1^{(2)}$, B_1 and B_2) are observed for the $W(CO)_4$ fragment of which the $A_1^{(2)}$ and B_1 overlap with the $Cr(CO)_3$ E band (complexes **4**, **6**).

ACCEPTED MANUSCRIPT

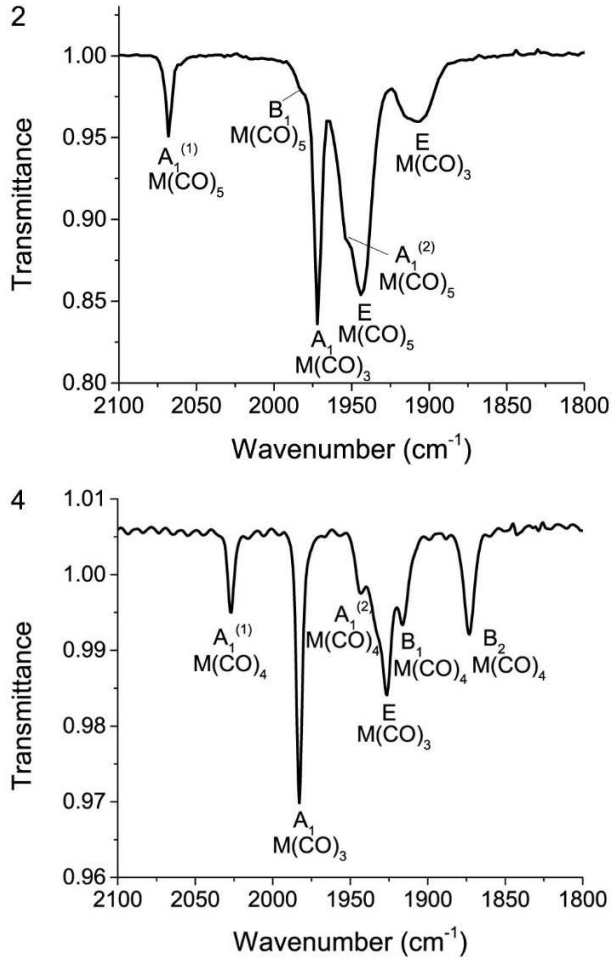

Figure 5. FT-IR spectra of **2** (top) and **4** (bottom) in the carbonyl region, recorded in hexane at 298 K

In the infrared spectrum of **7**, the $Cr(CO)_3$ bands are very weak and poorly resolved because of the presence of two $W(CO)_5$ fragments (Figure S-18, SI). Also, the IR spectrum displays two sets of $W(CO)_5$ bands with different intensities. The duplication of the bands is ascribed to the simultaneous occurrence of two different isomeric forms (Figure 6) in solution because of hindered rotation around the arene-carbene bonds. No duplication of signals is observed in the

NMR spectra, though, even at T = 230 K, and the syn isomer is obtained in the solid state as indicated by X-ray diffraction studies (*vide infra*).

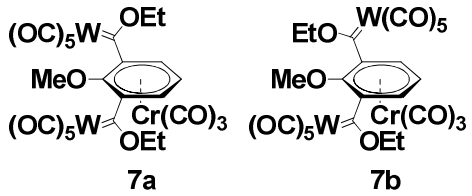

Figure 6. *Syn*- and *anti*-isomers proposed for **7**

3.4 Single Crystal X-Ray Structures. Single crystals of all complexes **1-7** were obtained by careful layering of concentrated solutions of the complexes in CH_2Cl_2 with hexane and their solid-state structures have been established by single crystal X-ray diffraction. Tables S-1 and S-2 of the SI list the most relevant bond lengths, bond angles and torsion angles. Experimental details and crystal and refinement data are collected as Tables S-3 and S-4 of the SI, and the ORTEPs of all structures are displayed in Figures 7, 9, and 10. The Cr atoms are in a pseudo-tetrahedral environment as is typical of three-legged piano stool $\{\eta^6$-arene$\}Cr(CO)_3$ complexes. The carbonyl and carbene fragments atoms adopt the expected octahedral coordination geometry at W.

ACCEPTED MANUSCRIPT

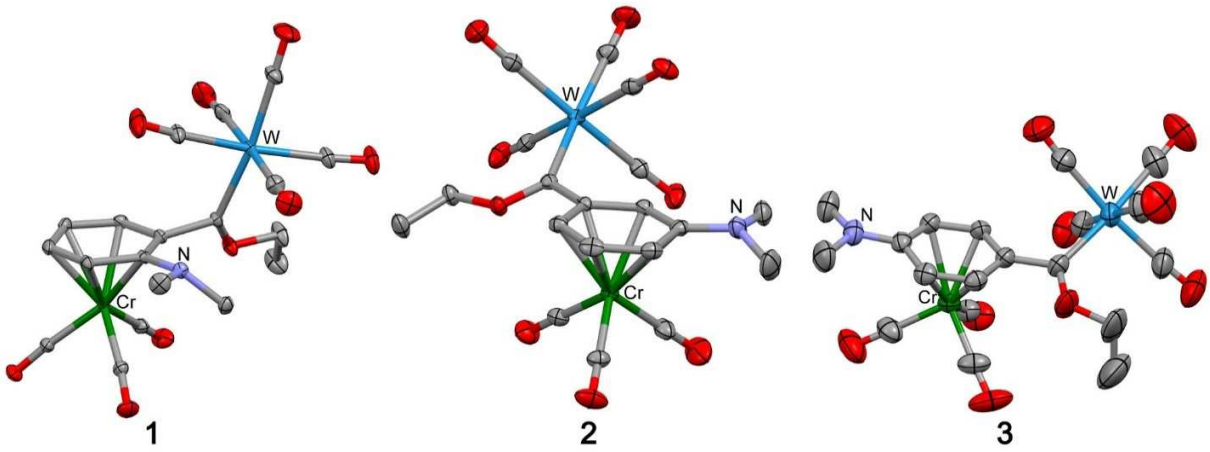

Figure 7. ORTEPs [40] of complexes **1-3**. Ellipsoids are set at 50% probability and hydrogen atoms are omitted for clarity

The molecular structures of the three positional isomers of {μ,$\eta^{6:1}$-$NMe_2C_6H_4C(OEt)W(CO)_5$}$Cr(CO)_3$ nicely illustrate the impact of the steric and electronic influences of the *N*,*N*-dimethylamine donor and the carbene acceptor. In the *p*-isomer **3**, these bulky substituents are sufficiently remote so as to allow for their more or less coplanar arrangement with the arene plane as indicated by interplanar angles of 1.8° of the NC_3 plane and of 22.2° of the carbene fragment (as defined by the atoms W,$C_{carbene}$,C_{aryl},O) with respect to the plane of the π-coordinated arene ligand. This allows for efficient resonance stabilization between the *p*-disposed donor and acceptor substituents. The near planarization of the nitrogen N atom with a C–N–C angle sum of 358.7°, the relatively short C_{arene}–N and C_{arene}–$C_{carbene}$ bonds of 1.354(3) and 1.485(3) Å and the noticeable quinoidal distortion of the η^6-arene ring with opposing short sides flanked by longer C–C bonds (see Figure 8) are clear indications of resonance interactions between *p*-disposed π-donor/π-acceptor substituents as is the relatively longer $C_{carbene}$–O bond of 1.327(4) Å. Less efficient resonance stabilization in the *m*-isomer **2** is

then indicated by a higher degree of pyramidalization of the N atom with the C–N–C angle sum of 354.0 or 354.5°, the longer C_{arene}–N and C_{arene}–$C_{carbene}$ bonds of 1.357(5) or 1.362(5) and 1.502(5) or 1.504(5) Å, and the shorter $C_{carbene}$–O bond of 1.305(4) or 1.314(4) Å for the two independent molecules of the unit cell. We also note the increased rotation of 8.1 or 8.9 and 27.3 or 27.5° of the amine and the carbene planes with respect to the plane of the π-coordinated arene ligand. As in **3**, the sterically demanding $W(CO)_5$ fragment points away from the $Cr(CO)_3$ entity.

Steric congestion between the bulky neighbouring NMe_2 and W{C(OEt)(aryl)} substituents hampers resonance interactions in the *o*-isomer **1**. Both these substituents are forced out of coplanarity with the arene ring and are rotated by 41.7° for the amine and by 70.2° for the tungsten carbene. With an angle sum of 347.2°, **1** shows the largest degree of pyramidalization of the aryl-NMe_2 substituent and the longest C_{arene}–N bond of 1.387(3) Å of all isomers. The bond lengths C_{arene}–$C_{carbene}$ and $C_{carbene}$–O of 1.494(3) and 1.318(2) Å are nevertheless very similar to **2**.

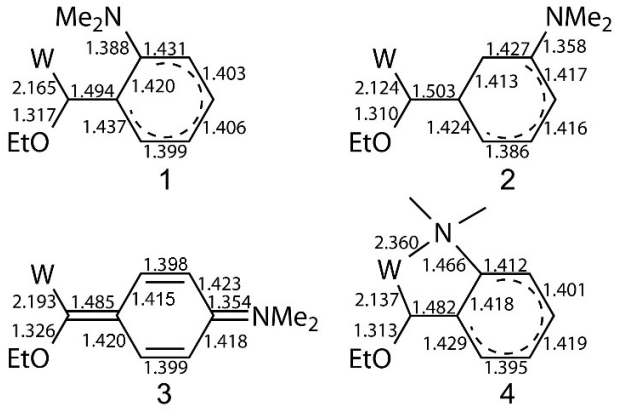

Figure 8. Bond distances (Å) [standard deviations are 0.002–0.004 Å (W–C), and 0.003–0.005 Å (all other bonds)] in the η^6-coordinated arene rings and at the carbene carbons showing areas of delocalization for **1** and **2** and alternating

long-short C–C_{arene} bonds of **3**. Bond distances shown for **2** are mean values for the two independent molecules in the structure.

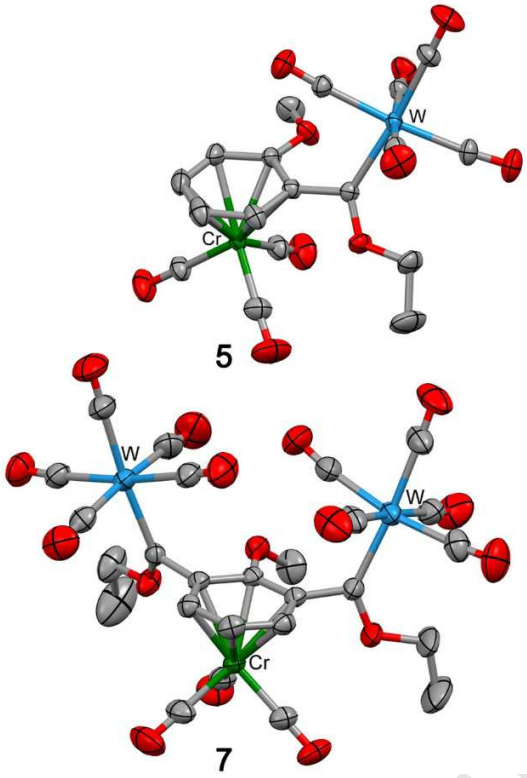

Figure 9. ORTEPs [40] of compounds **5** and **7**. Ellipsoids are set at 50% probability and hydrogen atoms omitted for clarity. Selected bond lengths [Å]: W–C_{carb} (**5**) 2.168(2), (**7**) 2.141(2), 2.144(3); C_{Ph}–C_{carb} (**5**) 1.503(3), (**7**) 1.504(3), 1.503(3); C_{carb}–OEt (**5**) 1.316(3), (**7**) 1.301(3), 1.308(3) and torsion angles [°]: W–C_{carb}–C_{ipso}–C_{Ph} (**5**) 60.6(2), (**7**) 102.3(2), –78.2(3); OEt–C_{carb}–C_{ipso}–C_{Ph} (**5**) 54.1(2), (**7**) 114.0(2), –76.9(3)

Owing to the presence of only one methyl substituent at the heteroatom and less steric hindrance, the rotation of the carbene fragment in the anisole complex **5** is decreased to 59.1° (Figure 9). As expected, the methoxy methyl group points away from the W{C(OEt)(aryl)}

fragment and the carbene fragment is poised above the arene ring, *anti* to the $Cr(CO)_3$ group. These structural features are retained in the heterotrimetallic biscarbene complex **7**. Increased steric congestion, however, causes an even larger torsion of the W{C(OEt)(aryl)} entities of 72.9 and 79.2° out of the plane of the attached π-coordinated arene ligand. Different to **5**, the methoxy methyl group is also forced out of the arene plane and points towards the $Cr(CO)_3$ fragment in order to avoid steric hindrance with the nearby carbene fragments. The $C_{carbene}$–O and W–$C_{carbene}$ distances in **7** of 1.301(3) and 1.308(3) or 2.142(2) and 2.144(3) Å are shorter than those of 1.316(3) or 2.168(2) Å in **5**, indicating greater contribution of the $W(CO)_5$ and OEt substituents in stabilizing the carbene centers in the σ,σ,π-trimetallic biscarbene complex.

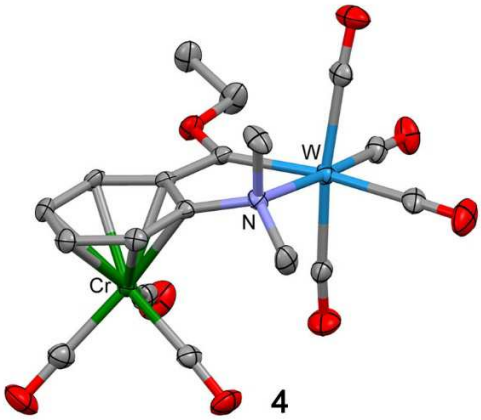

4

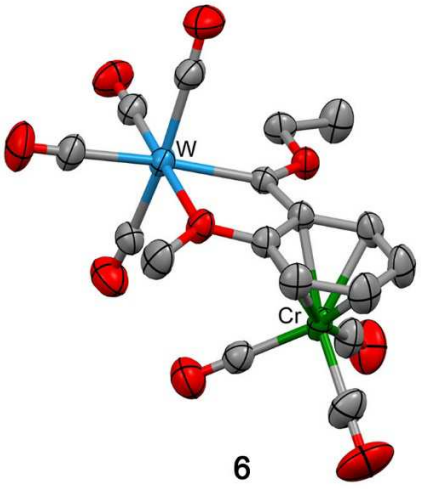

6

Figure 10. ORTEPs [40] of the σ,π-coordinated bimetallic carbene complexes **4** and **6**. Ellipsoids are set at 50% probability for σ,π-coordinated bimetallic carbene complexes. Hydrogen atoms omitted for clarity

Coordination of the heteroatom in the π-coordinated arene rings of **4** and **6** to W following carbonyl substitution affords scarce examples of σ,π-coordinated heterobimetallic chelate complexes. The W coordinated chelate ring (*C,N* in **4** or *C,O* in **6**, see Figure 10) enforces an acute chelate bite angle at W of 75.7(1)° for **4** and 73.7(1)° for **6** and shares an arene C–C bond with the π-coordinated $Cr(CO)_3$ moiety. In **6**, the five-membered chelate ring is nearly planar with only a slight fold of 3.8° at the carbene C and methoxy O atoms and the best plane through W and the four equatorial donors forms an interplanar angle of just 5.6° with the π-coordinated arene ring. In **4**, the five-membered ring adopts a half-chair conformation, which produces a fold of 15.5° between the equatorial coordination plane at W and the arene ring at the N and carbene C atom hinges. The methoxy methyl substituent of the anisole lies in the plane of the rings, while the two methyl groups of the dimethylaniline are locked in positions above and below the plane of the metallacyclic ring in line with the duplication of signals in the NMR spectra of **4**. On *N*-coordination, the angles around N become closer to 109° (116.8(1)°, 112.6(1)°, 105.3(2)° and 107.1(2)°), indicating sp^3 hybridization. This also results in a longer $N–C_{arene}$ distance of 1.466(3) Å compared to the value of 1.388(3) Å in **1**. By contrast, the oxygen of the anisole ring of **6** is in a trigonal planar environment as indicated by bond angles of 116.7(2)°, 118.6(2)°, 123.8(2)° and an angle sum of 359.1°.

The π-coordinated arene ligand of most complexes shows a slight boat- (complexes **1**, **3**, **7**) or chair-like (**5**, **7**) distortion with a fold of 3.5 to 11.2° as has been observed for numerous π-

coordinated complexes.[8,41,42] The maximum deviation from planarity is observed for **3**. The distance of the Cr atom to the aromatic plane scales with the electron density of the arene ring [42] and decreases from complexes **1**-**3** (1.729 to 1.738 Å) to complexes **5** and **7** (1.707 and 1.716 Å) and the methoxy chelate complex **6** (1.710 Å) to the amine chelate **4** (1.695 Å).

Figure S-19 in the SI displays the orientation of the carbonyl tripod with respect to a disubstituted arene ring along a C_3-axis perpendicular to the plane of the arene ring. Depending on the substituents, conformations are found that either eclipse (E) ring carbons or are staggered (S) between them. For the electron withdrawing carbene substituent (π-acceptor), an eclipsed conformation of the *o*- and *p*-carbons is expected while for an electron donating amino or methoxy substituent (π-donor), the *ipso*-carbon of the substituent and *m*-carbons should be eclipsed.[43,44] In agreement with these guidelines, the three complexes **3**, **5** and **6** display E-conformations. However, the *m*-substituted complex **2** or those compromised by bulky substituents (**1**, **4**, **7**) display S-conformations.[45]

3.5 Electrochemistry, Spectroelectrochemistry and Quantum Chemistry. Half wave potentials $E_{1/2}$ for the one-electron oxidation of a large number of {η^6-arene}$Cr(CO)_3$ complexes have been reported and were found to be sensitive to the electronic properties of the substituent(s) on the arene ring.[46–49] A pronounced anodic shift of $E_{1/2}$ with an increasingly electron withdrawing / lesser electron donating character of R in ring-substituted derivatives {η^6-RC_6H_5}$Cr(CO)_3$ (R = NMe_2, $E_{1/2}$ = 0.117 V; R = OMe, $E_{1/2}$ = 0.323 V; R = CO_2Me, $E_{1/2}$ = 0.587 V on the ferrocene/ferrocenium scale [50]) has been reported by Hunter and co-workers.[47] An intermediate value of 0.261 V was observed for the complex of 1,4-disubstituted *p*-$NMe_2C_6H_4CO_2Me$ with one electron donating and one electron withdrawing substituent,

showing that the effects of different substituents add up, albeit in a non-linear fashion if strong π-donor substituents like OMe or NR_2 are present.

Cyclic voltammograms of **1**-**7** were recorded in CH_2Cl_2 with NBu_4PF_6 as the supporting electrolyte. Table 2 lists the half wave or peak potentials of all observed processes against the ferrocene/ferrocenium standard. Inspection of the voltammograms in Figure 11 and Figures S-20 to S-26 of the SI reveals that all complexes undergo two consecutive oxidations. For complexes **1**-**5** the first oxidation constitutes a chemically reversible or partially reversible process (see inserts), while it is chemically irreversible for complexes **6** and **7**. Chemically irreversible behaviour also prevails for the second oxidation of every complex. With the exception of complex **3** all heterodi- and -trinuclear complexes with one or two $W(CO)_5$ carbene substituents also exhibit a reduction close to the cathodic limit of the supporting electrolyte. For **3**, which is clearly the most electron-rich representative of this series,[47] the reduction lies outside the breakdown limit of the solvent. Engagement of the heteroatom lone pair in metal coordination in chelate complexes **4** and **6** stabilises the associated radical anions and renders the reduction partially reversible (**6**) or even chemically reversible (**4**), while it constitutes a chemically irreversible process for all other complexes.

ACCEPTED MANUSCRIPT

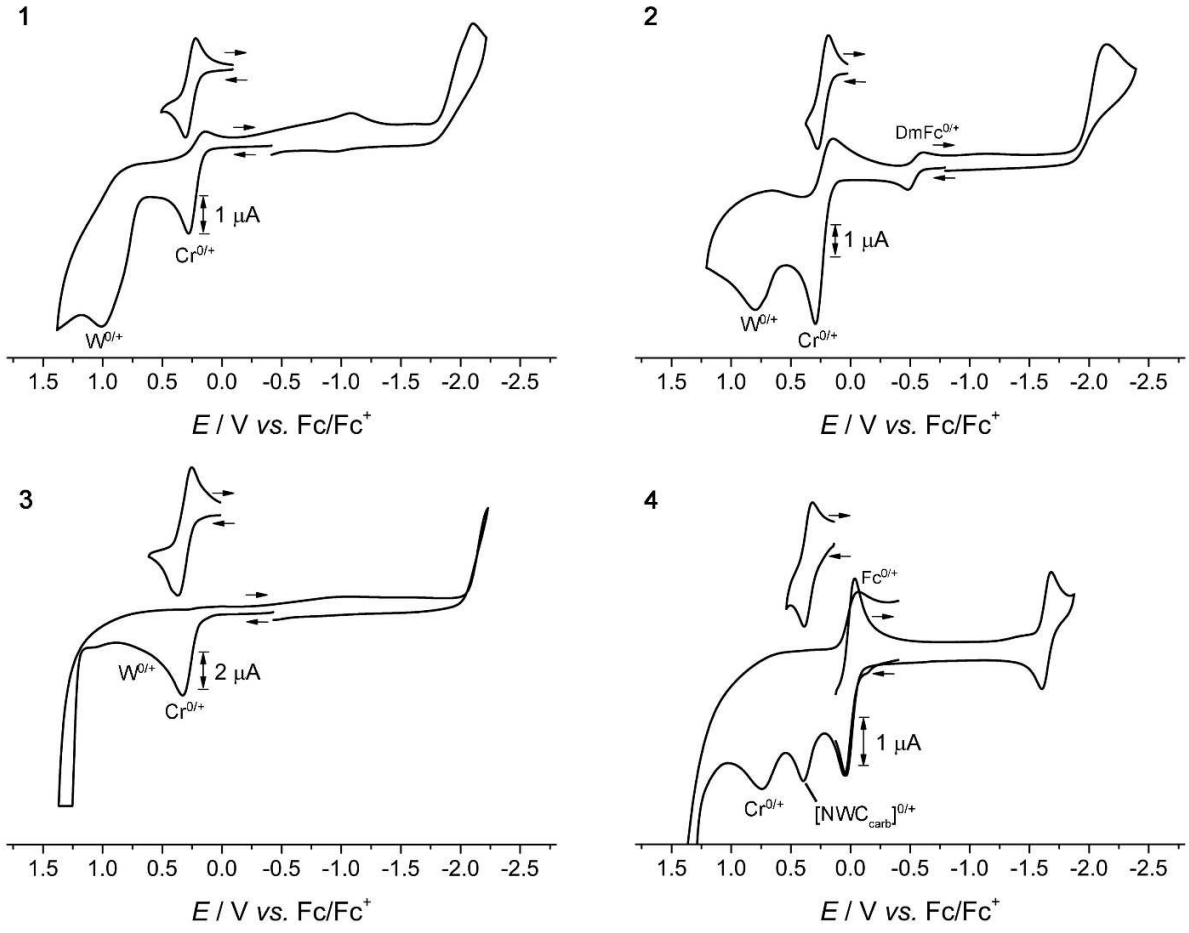

Figure 11. Cyclic voltammograms of complexes **1-4** in CH_2Cl_2/0.1 M NBu_4PF_6 against the ferrocene/ferrocenium standard at v = 100 mV/s

In agreement with literature data the first oxidation of the complexes **1-3** and **5** can be assigned to the $\{\eta^6$-arene$\}Cr(CO)_3$ moiety.[42,51,52] This was also confirmed by IR spectroelectrochemistry and DFT calculations. Thus, the HOMO of these complexes is strongly biased or entirely based on the $\{\eta^6$-arene$\}Cr(CO)_3$ unit (see Figure 12 and Figure S-31 of the SI). By comparing the half-wave potentials of the three isomeric complexes **1-3** we note that the *p*-isomer **3**, where the NMe_2 donor and the $(CO)_5W\{C(OEt)(aryl)\}$ carbene acceptor interact most

efficiently through π-resonance, oxidises at ca. 30 mV higher potential than the *o*- and *m*-isomers **1** and **2**. Such behaviour has been previously noted for the corresponding isomers of other disubstituted {η^6-(D)C_6H_4(A)}$Cr(CO)_3$ complexes with one donor (D) and one acceptor (A) substituent.[47] Replacement of the strong NMe_2 by the weaker OMe donor causes the expected anodic shift of $E_{1/2}$ by 109 mV (c. f. complexes **1** and **5**). Comparison of the half-wave potentials of complexes **1**-**3** with those of {η^6-1,4-$NMe_2C_6H_4CO_2Me$}$Cr(CO)_3$ ($E_{1/2}$ = 0.261 V) and {η^6-1,3-$NH_2C_6H_4CO_2Me$}$Cr(CO)_3$ ($E_{1/2}$ = 0.254 V) denotes the tungsten carbene as a similarly powerful electron acceptor as the ester substituent.

The second oxidation of complexes **1**, **2** and **5** is assigned to the expected $W^{0/+}$ oxidation of the arylC(OEt)$W(CO)_5$ carbene entity. Thus, complexes {2-thienylC(OEt)$W(CO)_5$} and {2-furylC(OEt)$W(CO)_5$} oxidise at an anodic peak potential of 0.728 and 0.697 V, respectively, under similar conditions.[41] The irreversible reduction of the present complexes agrees with the known behaviour of other {η^6-arene}$Cr(CO)_3$ [53–55] derivatives (c. f. E_p^a = -1.59 V for {η^6-$OMeC_6H_5CO$}$Cr(CO)_3$, considering the 400 mV potential difference between the Ag/AgI and the Fc/Fc^+ scales [56]), but also with that of Fischer type carbene complexes [16,57,58] (c. f. E_p^c = -1.564 V for {2-thienylC(OEt)$W(CO)_5$} and -1.645 V for {2-furylC(OEt)$W(CO)_5$}. While this makes an *a priori* assignment of the primary reduction site in the present complexes impossible, our quantum chemical calculations indicate that the LUMO of every complex is either biased towards the {arylC(OEt)$W(CO)_5$} entity or delocalised over the entire molecule. Graphical accounts of the relevant frontier MOs are displayed in Figure 12 for complexes **1**-**4**, and in Figure S-31 of the SI for complexes **5**-**7**. We nevertheless note that substitution of the NMe_2 (complex **1**) by the OMe substituent (complex **5**) causes a similar anodic displacement of the reduction potential as it was observed for the oxidation.

Substitution of one carbonyl ligand at the tungsten carbene by the lone pair of the heteroatom substituent is expected to shift the oxidation potential of that moiety to lower values, similar to what has been observed in metal tetracarbonyl phosphine complexes.[59,60] At the same time it will increase the oxidation potential of the substituted {η^6-arene}$Cr(CO)_3$ moiety as the heteroatom lone pair is no longer available for resonance interaction with the π-coordinated arene ligand and the previous NMe_2 or OMe donor has evolved to a net acceptor. The finding that the oxidation potential of chelate complex **4** is by 128 mV higher than that of its precursor **1** matches with both expectations, thus precluding an *a priori* assignment of the first oxidation to either the tungsten carbene or the {η^6-arene}$Cr(CO)_3$ unit. The first oxidation potential of the related chelate complex **6** is likewise shifted anodically with respect to that in **5**. Although the chemical irreversibility of this process in complex **6** precludes a strict comparison of the magnitude of the shift on chelation between the pairs of complexes **1**/**4** and **5**/**6**, it seems to be rather similar in both cases. Our quantum chemical calculations argue for a tungsten carbene-centered process, as the HOMO of complexes **4** and **6** is clearly dominated by that entity (Figure 12 and Figure S-31 of the SI). This finds also support from our spectroelectrochemical studies (*vide infra*). CO substitution and *N*- or *O*-chelation by the heteroatom substituent also induces a sizable anodic shift of the reduction potentials and renders the immediate reduction products chemically more stable when compared to their $W(CO)_5$ precursors. This is only compatible with a {η^6-arene}$Cr(CO)_3$-based reduction process for both complexes and also matches with the results of our quantum chemical calculations.

Table 2. Oxidation and reduction half-wave or peak potentials of complexes **1-4** and **5-7** in CH_2Cl_2/0.1 M NBu_4PF_6 against the ferrocene/ ferrocenium standard

	1st Oxidation				2nd Oxidation	Reduction
	E_{pc} / V	E_{pa} / V	ΔE_p / V [i_{pc}/i_{pa}]	$E_{1/2}$ / V	$E_p{}^a$ / V[a)]	E / V
1	0.194	0.280	0.086 [0.80]	0.237	1.011	-2.102[a)]
2	0.185	0.274	0.089 [1.00]	0.232	0.796	-1.2.142[a)]
3	0.208	0.324	0.116 [0.96]	0.264	n.o.	n. o.
4	0.376	0.441	0.065 [0.70]	0.355	0.737	-1.643
5	0.308	0.384	0.076 [0.69]	0.346	0.904	-2.012[a)]
6	–	0.545[a)]	–	–	0.742	-1.781[a)]
7	–	0.518[a)]	–	–	0.960[b)]	-1.951[a)]

a) Peak potential of a chemically irreversible process. b) Additional anodic peak at Ep = 0.727 V

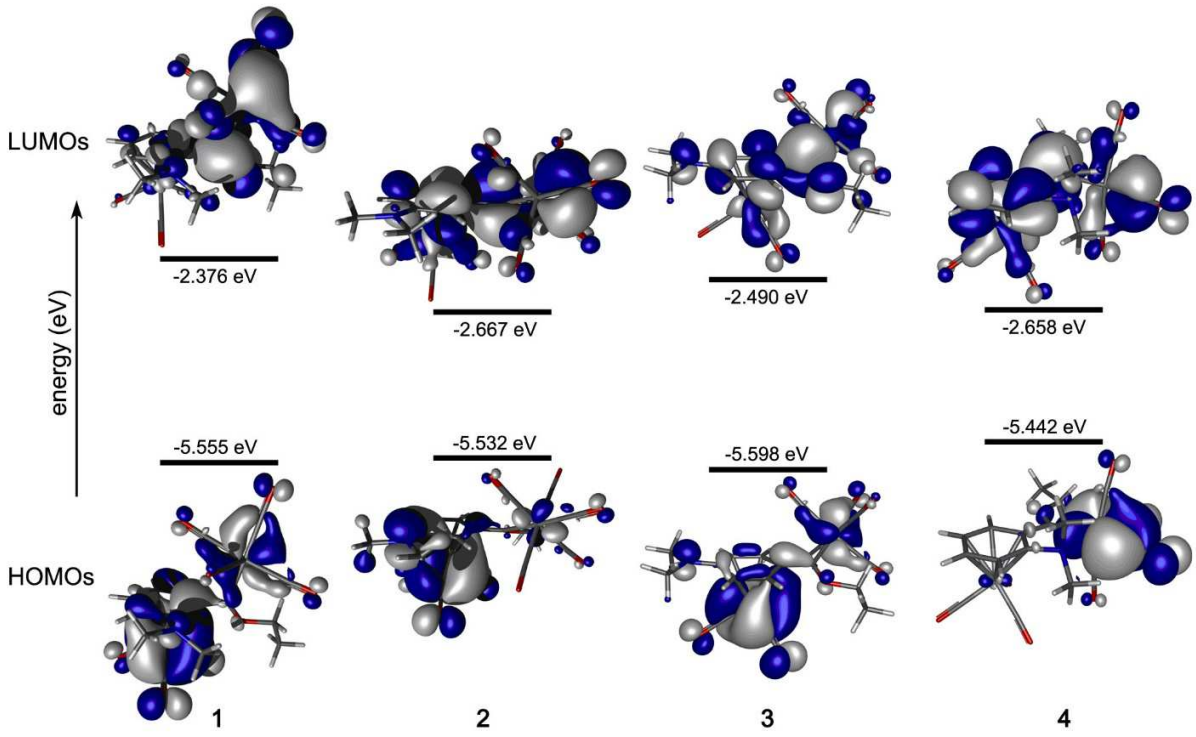

Figure 12. Contour plots and energies of the calculated HOMO and LUMO orbitals of the neutral complexes **1-4**

Despite the chemical reversibility of their one-electron oxidations under the conditions of cyclic voltammetry, radical cations of complexes $\{\eta^6\text{-}RC_6H_5\}Cr(CO)_3$ have long remained elusive due to their high inherent reactivity.[42,46,52,61–63] This problem was ultimately solved with the advent of supporting electrolytes with very weakly nucleophilic BAr_F^--type anions such as $B(C_6F_5)_4^-$ or $B\{2,5\text{-}C_6H_3(CF_3)_2\}^-$. Using these electrolytes, Geiger and co-workers could establish that oxidation of such complexes produces an average-weighted shift (the doubly degenerate asymmetric band has to be counted twice) of ν(CO) by ca. 115 cm^{-1}, in line with a metal-centred oxidation of a carbonyl complex. A slightly decreased average-weighted shift of 109 cm^{-1} was noted for the $\{\eta^6\text{-}C_6Et_6\}Cr(CO)_3^{0/+}$ redox couple.[61,62] Here, the combined effects of higher electron density and steric protection rendered the radical cation accessible even in the presence of the conventional NBu_4ClO_4 supporting electrolyte.[64] This is also in line with quantum chemical results of such complexes, which assign the HOMO as primarily the Cr d_z^2 orbital.[65]

Oxidation of complexes **1, 2** and **4** proceeded smoothly inside a transparent thin-layer electrolysis cell [17] with the $1,2\text{-}C_2H_4Cl_2$ / NBu_4PF_6 electrolyte as indicated by the multiple isosbestic points. Only partial conversion could, however, be achieved for **3** before the onset of irreversible chemical changes. Graphical accounts of these experiments are compiled in Figure 13 and Figures S-27 and S-28 of the SI while Table 3 and Table S-5 of the SI list the values of ν(CO) as extracted from digital deconvolution of the experimental spectra (see Figures S-29 and S-30 of the SI). For complexes **1** and **2**, one-electron oxidation causes sizable blue shifts of the ν(CO) bands of the $Cr(CO)_3$ entity with an average shift value of 64 cm^{-1} for **1** and a smaller value of 49 cm^{-1} for **2**. Due to only partial conversion of **3** to its associated radical cation, only

the shift of the A_1 band from 1959 cm^{-1} to 1996 cm^{-1} can be safely reported; this value is similar to, but even smaller than that for the **2**/**2**$^+$ redox pair. Quite revealingly, though, there is an only minor shift of the $A_1^{(1)}$, $A_1^{(2)}$ and E bands of the $W(CO)_5$ moiety of just about 5 cm^{-1}, which reflects a subordinate contribution of the carbene center to one-electron oxidation. We nevertheless note that the CO band shifts of the $Cr(CO)_3$ unit are considerably smaller than those previously reported for parent $\{\eta^6\text{-}C_6H_6\}Cr(CO)_3$ and its hexaethyl or a disubstituted estradiol derivative.[61,62,64] This signals an unusually large contribution of the π-arene ligand to the relevant redox orbital and the ability of the NMe_2 donor and tungsten carbene "substituents" to act as electron buffers. This notion finds support from our quantum chemical calculations, which indicate non-negligible contributions of the NMe_2 substituents and the d_{xy} orbital of W to the HOMO (Figures 12 and S-31 of the SI). The latter orbital is roughly coplanar to the arene plane. Comparison of the frontier MOs of the neutral complexes in Figures 12 and S-31 of the SI with those of their associated oxidised forms in Figures S-32 and S-33 of the SI indicate that the level ordering of the neutral complex **1**-**3** is retained in their oxidised forms and that the spin density almost exclusively resides at the $Cr(CO)_3$ fragment.

Extensive overlap of the E band of the $Cr(CO)_3$ and the $A_1^{(2)}$, B_1 or the B_2 bands of the $W(CO)_4$ entities preclude a meaningful assignment of every vibrational band of either **4** and **4**$^+$. More substantial blue shifts of the characteristic $A_1^{(1)}$ and B_2 bands of $W(CO)_4$ and the rather minor shifts of the A_1 and E bands of $Cr(CO)_3$ nevertheless allow us to assign the first oxidation to the $\{C,N\text{-}o\text{-}NMe_2C_6H_4C(OEt)W(CO)_4\}$ entity. The latter assignment is in line with the trends in cyclic voltammetry and is also supported by our quantum chemical calculations. Thus, the HOMO of complexes **4** and **6** is almost exclusively based on the tungsten carbene, as is the spin density of their associated radical cations (see Figures 12, and S-31 to S-33). Table S-6 provides

computed IR peaks at unscaled energies. Experimental trends for the non-chelated complexes are qualitatively well reproduced. In particular, the bands that can be identified as originating from the $Cr(CO)_3$ group show substantially larger blue shifts than those of the $W(CO)_5$ moiety. For the $W(CO)_4$-containing chelate complexes, no straightforward analysis is, however, possible due to extensive overlap of the individual bands and the fact that our calculations fail to localise the various modes at a particular $M(CO)_n$ entity.

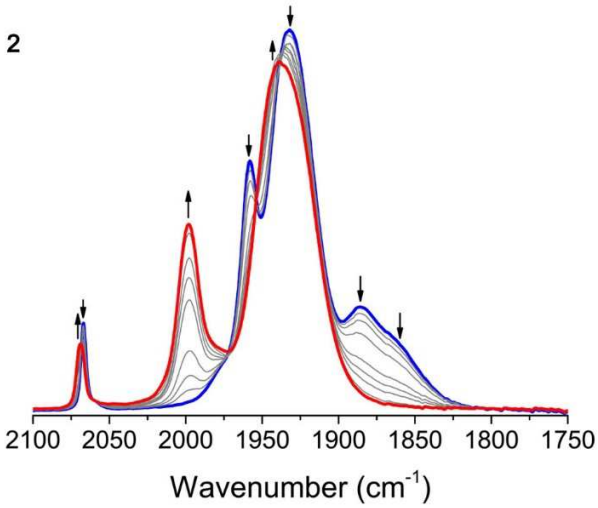

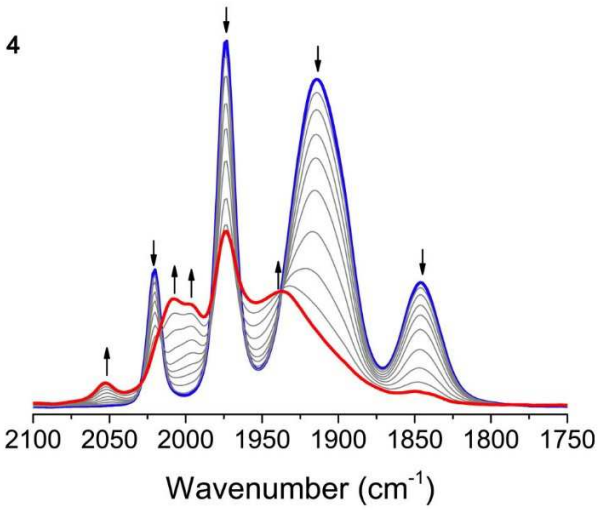

Figure 13. IR spectroscopic changes upon the oxidation of complexes **2** and **4** inside an OTTLE cell (1,2-$C_2H_4Cl_2$/NBu_4PF_6, 298 K)

Table 3. ν(CO) band positions (in cm^{-1}) of complexes **1-4** in their neutral and oxidised states in 1,2-$C_2H_4Cl_2$/NBu_4PF_6 (0.1 M) as electrolyte at 298 K

	[Cr(CO)$_3$]		**[W(CO)$_5$]**			
	A_1	**E**	**$A_1^{(1)}$**	**B_1**	**$A_1^{(2)}$**	**E**
1	1943(vs)	1880(br)	2072	1988(vw)	1943(vs)	1943(vs)
1^+	1994(s)	1950(vs)	2080	n.o.	1950(vs)	1950(vs)
2	1958(s)	1886(br)	2067	1977(w)	1932(vs)	1932(vs)
2^+	1998(s)	1939(vs)	2068	n.o.	1939(vs)	1939(vs)

	[Cr(CO)$_3$]		**[W(CO)$_4$]**			
	A_1	**E**	**$A_1^{(1)}$**	**$A_1^{(2)}$**	**B_1**	**B_2**
4	1973(vs)	1915(vs)	2020	n.o.	1915(vs)	1846
4^+	1973(vs)	1937(br)	2052	2009	1945	n.o.

4. Summary and Conclusion.

In this study heterobi- and -trimetallic Cr(0), W(0) Fischer ethoxycarbene complexes, where one or two {C(OEt)$W(CO)_5$}-type tungsten carbenes are σ-bonded to a {η^6-RC_6H_4}$Cr(CO)_3$ or a {η^6-RC_6H_3}$Cr(CO)_3$ entity, were successfully synthesised from their corresponding {η^6-RC_6H_5}$Cr(CO)_3$ precursors. π-Coordination to $Cr(CO)_3$ of *N*,*N*-dimethylaniline resulted in an enhanced activation of all ring positions. Hence, it was possible to isolate all three positional isomers of the heterobimetallic carbene complexes. In the mono- and biscarbene complexes **5**

and **7** of the π-coordinated anisole, the carbene fragments are exclusively in the *o*-position(s) relative to the ring methoxy substituent. For both the *o*-monocarbene complexes, the lone pair of the amine or the methoxy donor can replace a carbonyl ligand on the W centre to form an annulated 5-membered chelate ring.

Through spectroscopic, structural, electrochemical and theoretical studies it was shown that the *N*,*N*-dimethylamine, methoxy and tungsten carbene substituents have a marked influence on the electron density at the π-coordinated arene and hence the $Cr(CO)_3$ group. The greater π-electron density of *N*,*N*-dimethylaniline when compared to anisole was revealed in the distances between the center of the arene ring and the Cr atom of the $Cr(CO)_3$ group in the solid-state structures of the compounds as well as in their electrochemical data. The position of the carbene substituent relative to the amine substituent in the *N*,*N*-dimethylaniline also has an influence. The *p*-isomer displays the greatest delocalization of the electron lone pair, followed by the *m*- and *o*-isomers, respectively. Steric crowding between the ring substituents in the *o*-disubstituted complexes **1**, **5**, and **7** precludes efficient orbital overlap between the NMe_2 or the OMe donor and the tungsten carbene acceptor. The primary oxidation sites within these heterobi- and -trimetallic complexes were assigned as $(\eta^6\text{-}RC_6H_3)Cr(CO)_3$ for complexes **1**-**3**, **5** and **7**, and as the {*C*,*N*-*o*-$NMe_2C_6H_4C(OEt)W(CO)_4$} or the {*C*,*N*-*o*-$OMeC_6H_4C(OEt)W(CO)_4$} entity in chelate complexes **4** and **6**. These assignments were derived from the trends in electrochemical oxidation and reduction potentials and are confirmed by quantum chemical calculations and, experimentally, by IR spectroelectrochemistry. As to the latter we note that we successfully generated and characterised radical cations $\mathbf{1}^+$, $\mathbf{2}^+$ and $\mathbf{4}^+$.

ASSOCIATED CONTENT

Accession Codes: CCDC 1577569, CCDC 1577570, CCDC 1577571, CCDC 1577572, CCDC 1577573, CCDC 1577574 and CCDC 1577575 contains the supplementary crystallographic data for this paper. This data can be obtained free of charge via www.ccdc.cam.ac.uk/data_request/cif, or by emailing data request@ccdc.cam.ac.uk, or by contacting The Cambridge Crystallographic Data Centre, 12 Union Road, Cambridge CB2 1EZ, UK; fax: +44 1223 336033.

Supplementary data: Supplementary data related to this article can be found at … Experimental details including NMR, IR, Crystallographic data and results from DFT calculations, graphical representations of spectra, cyclic voltammograms, IR-SEC experiments along with spectral deconvolutions and graphical representations of relevant frontier MOs of the neutral complexes and their associated radical cations along with spin density plots and calculated IR frequencies and band assignments; tables with the atomic coordinates of the geometry-optimized structures from DFT calculations. The CIF files corresponding to the X-ray structures have been deposited at the Cambridge Structure Data Base as CCDC 1577569 to CCDC 157575 and can be obtained free of charge via www.ccdc.cam.ac.uk/conts/retrieving.html or from the Cambridge Crystallographic Data Center, 12 Union Road, Cambridge CB2 1EZ, U.K.; fax (+44)1223-336-033, or at deposit@ccdc.cam.ac.uk.

Corresponding Authors

*Corresponding Authors: SL: simon.lotz@up.co.za, RW: rainer.winter@uni-konstantz.de

ORCID:

Nora-ann Weststrate: 0000-0003-0393-2973

Christopher Hassenrück: 0000-0002-2506-7530

Rainer F. Winter: 0000-0001-8381-0647

Notes

The authors declare no competing financial interest.

Acknowledgment

SL acknowledges the Alexander von Humboldt Foundation and University of Pretoria for funding of a research visit in Konstanz and the NRF for financial support of the project by GUN 87788 and 95772 grants. NW and SL kindly acknowledge the LC-MS Synapt Facility (Department of Chemistry, University of Pretoria) for mass spectrometry services provided by Ms Madelien Wooding and some help in obtaining NMR spectra by Ms Zandria Lamprecht. NW gratefully acknowledges financial support by the University of Pretoria and the NRF for a research visit to the Universität Konstanz and to Prof. Winter for hosting her on two occasions. RFW thanks the state of Baden-Württemberg, Germany, for providing access to the bwHPC computational facilities at the Karlsruhe Institute of Technology (KIT).

REFERENCES

[1] N. Kuhl, M.N. Hopkinson, J. Wencel-Delord, F. Glorius, Beyond directing groups: transition-metal-catalyzed C-H activation of simple arenes, Angew. Chem. Int. Ed. 51 (2012) 10236–10254.

[2] C.-L. Ciana, R.J. Phipps, J.R. Brandt, F.-M. Meyer, M.J. Gaunt, A highly *para*-selective copper(II)-catalyzed direct arylation of aniline and phenol derivatives, Angew. Chem. Int. Ed. 50 (2011) 458–462.

[3] N.F. Masters, D.A. Widdowson, Regiocontrolled lithiation of arenetricarbonylchromium (0) complexes: meta-substitution of phenols and anilines, J. Chem. Soc., Chem. Commun. (1983) 955–956.

[4] P. Ricci, K. Krämer, X.C. Cambeiro, I. Larrosa, Arene-metal π-complexation as a traceless reactivity enhancer for C-H arylation, J. Am. Chem. Soc. 135 (2013) 13258–13261.

[5] D. Prim, B. Andrioletti, F. Rose-Munch, E. Rose, F. Couty, Bimetallic Pd/Cr and Pd/Mn activation of carbon–halide bonds in organochromium and organomanganese complexes, Tetrahedron 60 (2004) 3325–3347.

[6] M. Rosillo, G. Domínguez, J. Pérez-Castells, Chromium arene complexes in organic synthesis, Chem. Soc. Rev. 36 (2007) 1589–1604.

[7] A. Berger, J.-P. Djukic, C. Michon, Metalated (η^6-arene)tricarbonylchromium complexes in organometallic chemistry, Coord. Chem. Rev. 225 (2002) 215–238.

[8] R. Meyer, M. Schindehutte, P.H. van Rooyen, S. Lotz, π-Arene Complexes. 10. Arene Distortions in π-Arene Complexes of Chromium by Ring Substituents. Crystal Structure of (η^1:η^6-C_6H_5{$TiCp_2Cl$})$Cr(CO)_3$, Inorg. Chem. 33 (1994) 3605–3608.

[9] R. Meyer, P.L. Wessels, P.H. van Rooyen, S. Lotz, π-Arene complexes: 11. Site control affected by steric and electronic factors of ring substituents in σ,π-coordinated bimetallic complexes, Inorg. Chim. Acta. 284 (1999) 127–132.

[10] D. Möhring, M. Nieger, B. Lewall, K.H. Dötz, Tricarbonyl(naphthoquinone)chromium: Synthesis and Application in [4+2] Cycloaddition Reactions, Eur. J. Org. Chem. (2005)

2620–2628.

[11] J.-P. Djukic, A. Maisse, M. Pfeffer, K.H. Dötz, M. Nieger, First synthesis and structural characterization of neutral chelated *syn-facial* bimetallic (η^5-cyclohexadienyl)benzylidene complexes from tetracarbonyl[2-{(η^6-phenyl)tricarbonylchromium(0)-κ*C*2′}pyridine-κ*N*]manganese(I) derivatives, Eur. J. Inorg. Chem. (1998) 1781–1790.

[12] D.I. Bezuidenhout, B. van der Westhuizen, N.A. van Jaarsveld, S. Lotz, Trends in the chemistry of mono- to multimetal π-arene complexes of chromium and manganese, J. Inorg. Organomet. Polym. 24 (2014) 39–57.

[13] E.O. Fischer, F.J. Gammel, D. Neugebauer, Übergangsmetall-Carbin-Komplexe, LII. (Tricarbonylchrom)-η^6-phenyl als Substituent in Carben- und Carbinkomplexen der VI. Nebengruppe, Chem. Ber. 113 (1980) 1010–1019.

[14] D.I. Bezuidenhout, E. van der Watt, D.C. Liles, M. Landman, S. Lotz, Steric and electronic effects of metal-containing substituents in Fischer Carbene complexes of chromium, Organometallics 27 (2008) 2447–2456.

[15] M.A. Sierra, Di- and polymetallic heteroatom stabilized (Fischer) metal carbene complexes, Chem. Rev. 100 (2000) 3591–3638.

[16] I. Hoskovcová, R. Zvěřinová, J. Roháčová, D. Dvořák, T. Tobrman, S. Záliš, J. Ludvík, Fischer aminocarbene complexes of chromium and iron: Anomalous electrochemical reduction of p-carbonyl substituted derivatives, Electrochim. Acta. 56 (2011) 6853–6859.

[17] M. Krejčik, M. Daněk, F. Hartl, Simple construction of an infrared optically transparent thin-layer electrochemical cell: applications to the redox reactions of ferrocene,

$Mn_2(CO)_{10}$ and $Mn(CO)_3$(3,5-di-*t*-butyl-catecholate)$^-$, J. Electroanal. Chem. 317 (1991) 179–187.

[18] TURBOMOLE 7.1, 2016, A development of University of Karlsruhe and Forschungszentrum Karlsruhe GmbH, 1989-2007, TURBOMOLE GmbH, since 2007; Available from Http://www.turbomole.com.

[19] F. Weigend, M. Häser, H. Patzelt, R. Ahlrichs, RI-MP2: optimized auxiliary basis sets and demonstration of efficiency, Chem. Phys. Lett. 294 (1998) 143–152.

[20] A. Hellweg, C. Hättig, S. Höfener, W. Klopper, Optimized accurate auxiliary basis sets for RI-MP2 and RI-CC2 calculations for the atoms Rb to Rn, Theor. Chem. Acc. 117 (2007) 587–597.

[21] F. Weigend, R. Ahlrichs, Balanced basis sets of split valence, triple ζ valence and quadruple ζ valence quality for H to Rn: design and assessment of accuracy, Phys. Chem. Chem. Phys. 7 (2005) 3297–3305.

[22] K. Kim, K.D. Jordan, Comparison of density functional and MP2 calculations on the water monomer and dimer, J. Phys. Chem. 98 (1994) 10089–10094.

[23] P.J. Stephens, F.J. Devlin, C.F. Chabalowski, M.J. Frisch, *Ab initio* calculation of vibrational absorption and circular dichroism spectra using density functional force fields, J. Phys. Chem. 98 (1994) 11623–11627.

[24] M. Cossi, N. Rega, G. Scalmani, V. Barone, Energies, structures, and electronic properties of molecules in solution with the C-PCM solvation model, J. Comput. Chem. 24 (2003) 669–681.

[25] A. Klamt, Conductor-like screening model for real solvents: a new approach to the quantitative calculation of solvation phenomena, J. Phys. Chem. 99 (1995) 2224–2235.

[26] C.A.L. Mahaffy, P.L. Pauson, M.D. Rausch, W. Lee, (η^6-Arene)tricarbonylchromium complexes, in Inorganic Synthesis: Reagents for transition metal complex and organometallic syntheses, Volume 28, John Wiley & Sons, Inc., 1990.

[27] K. Öfele, Ein neuer Weg zur Darstellung von Aromaten-Metall-Carbonylen, Chem. Ber. 99 (1966) 1732–1736.

[28] P.M. Treichel, R.U. Kirss, Metalation of the fused polycyclic aromatic ligand in (arene)chromium tricarbonyl complexes: kinetic and thermodynamic site preferences, Organometallics 6 (1987) 249–254.

[29] A.R. Lepley, W.A. Khan, A.B. Giumanini, A.G. Giumanini, Metallation of *N*,*N*-Dimethylaniline, J. Org. Chem. 31 (1966) 2047–2051.

[30] R.J. Card, W.S. Trahanovsky, Arene-metal complexes. 13. Reaction of substituted (benzene)tricarbonylchromium complexes with n-butyllithium, J. Org. Chem. 45 (1980) 2560–2566.

[31] D.I. Bezuidenhout, S. Lotz, D.C. Liles, B. van der Westhuizen, Recent advances in the field of multicarbene and multimetal carbene complexes of the Fischer-type, Coord. Chem. Rev. 256 (2012) 479–524.

[32] P. Ricci, K. Krämer, I. Larrosa, Tuning reactivity and site selectivity of simple arenes in C-H activation: ortho-arylation of anisoles via arene-metal π-complexation., J. Am. Chem. Soc. 136 (2014) 18082–18086.

[33] K.H. Dötz, W. Sturm, M. Popall, J. Riede, Carbenliganden als anthracyclinon-synthone I. methoxyarylcarbene als chelatliganden, J. Organomet. Chem. 277 (1984) 267–275.

[34] S. Lotz, M. van den Berg, J.L.M. Dillen, Metallocyclic carbene complexes of chromium(0). The crystal and molecular structure of a chronium(0) complex with an aminoarylcarbene chelating ligand, Trans. Met. Chem. 13 (1988) 170–175.

[35] E.O. Fischer, C.G. Kreiter, H.J. Kollmeier, J. Müller, R.D. Fischer, Übergangsmetall-carben-komplexe XXVII. Ringsubstituierte (Methoxyphenylcarben)-Pentacarbonylchrom(o)-Komplexe, J. Organomet. Chem. 28 (1971) 237–258.

[36] S.E. Gibson, H. Ibrahim, Asymmetric catalysis using planar chiral arene chromium complexes, Chem. Commun. (2002) 2465–2473.

[37] Y.M. Terblans, S. Lotz, π-Heteroarene Complexes. 4. Synthesis and structure of bimetallic complexes with σ,π-bridged thienyl monocarbene ligands, J. Chem. Soc., Dalton Trans. (1997) 2177–2182.

[38] P.S. Braterman, Metal Carbonyl Spectra, Academic Press Inc., London, 1975.

[39] K. Heinz Dötz, H.-G. Erben, W. Staudacher, K. Harms, G. Müller, J. Riede, Reaktionen von Komplexliganden, J. Organomet. Chem. 355 (1988) 177–191.

[40] L.J. Farrugia, WinGX and ORTEP for Windows: an update, J. Appl. Ctrystallogr. 45 (2012) 849–854.

[41] P. Le Maguères, S. V. Lindeman, J.K. Kochi, Electron redistribution of aromatic ligands in (arene)$Cr(CO)_3$ complexes. Structural (bond-length) changes as quantitative measures, Organometallics 20 (2001) 115–125.

[42] A.D. Hunter, V. Mozol, S.D. Tsai, Nonlinear substituent interactions and the electron richness of substituted (η^6-arene)$Cr(CO)_3$ Complexes as measured by IR and C^{13} NMR spectroscopy and cyclic voltammetry: role of π-donor and π-acceptor interactions, Organometallics 11 (1992) 2251–2262.

[43] E.L. Muetterties, J.R. Bleeke, E.J. Wucherer, T. Albright, Structural, stereochemical, and electronic features of arene-metal complexes, Chem. Rev. 82 (1982) 499–525.

[44] K. Schoellkopf, J.J. Stezowski, F. Effenberger, Aminobenzenes. 18. Crystal and molecular structures of novel (arene)chromium tricarbonyl complexes, Organometallics 4 (1985) 922–929.

[45] T.A. Albright, P. Hofmann, R. Hoffmann, Conformational preferences and rotational barriers in polyene-ML_3 transition metal complexes, J. Am. Chem. Soc. 99 (1977) 7546–7557.

[46] J.O. Howell, J.M. Goncalves, C. Amatore, L. Klasinc, R.M. Wightman, J.K. Kochi, Electron transfer from aromatic hydrocarbons and their π-complexes with metals. Comparison of the standard oxidation potentials and vertical ionization potentials, J. Am. Chem. Soc. 106 (1984) 3968–3976.

[47] A.D. Hunter, V. Mozol, S.D. Tsai, Nonlinear substituent interactions and the electron richness of substituted (η^6-arene)$Cr(CO)_3$ complexes as measured by IR and C^{13} NMR spectroscopy and cyclic voltammetry: role of π-donor and π-acceptor interactions, Organometallics 11 (1992) 2251–2262.

[48] F. Rourke, R. Gash, J.A. Crayston, Electrochemical generation of 17-electron cation

radicals from arene-$M(CO)_3$ (M = Cr, Mo, W) and thiophene-$Cr(CO)_3$ Complexes in MeCN: Conventional cyclic voltammetric studies with digital simulation and microelectrode voltammetry in the absence of supporting electrolyte, J. Organomet. Chem. 423 (1992) 223–239.

[49] M.K. Lloyd, J.A. McCleverty, J.A. Connor, E.M. Jones, Voltammetric oxidation of arene, cycloheptatriene, and cycloheptatrienyl tricarbonyl complexes of chromium, J. Chem. Soc., Dalt. Trans. (1973) 1768–1770.

[50] N.G. Connelly, W.E. Geiger, Chemical redox agents for organometallic chemistry, Chem. Rev. 96 (1996) 877–910.

[51] W.E. Geiger, One-electron electrochemistry of parent piano-stool complexes, Coord. Chem. Rev. 257 (2013) 1459–1471.

[52] P.G. Gassman, P.A. Deck, Tricarbonyl(η^6-hexachlorobenzene)chromium(0), Organometallics 13 (1994) 1934–1939.

[53] A. Garg, D.M. Nemer, H. Choi, J.B. Sheridan, W.E. Geiger, On the question of redox-induced haptotropic rearrangements in the electrochemical reduction of η^6-triolefin chromium complexes having nonaromatic ligands, Organometallics 25 (2006) 275–282.

[54] Y.L. Chiu, A.E.G. Sant'ana, J.H.P. Utley, Electro-organic reactions. Part 29: cathodic reduction activated by arene-chromium tricarbonyl complexation, Tetrahedron Lett. 28 (1987) 1349–1352.

[55] T.J.J. Müller, Redox active alkenyl-bridged bi- and trinuclear arene–$Cr(CO)_3$-complexes by Horner–Emmons–Wadsworth olefinations, J. Organomet. Chem. 578 (1999) 95–102.

[56] K. Isutzu, Electrochemistry in nonaqueous solutions, Wiley-VCH Weinheim, 2002.

[57] M. Landman, R. Pretorius, B.E. Buitendach, P.H. van Rooyen, J. Conradie, Synthesis, Structure, and Electrochemistry of Fischer Alkoxy- and Aminocarbene Complexes of Tungsten: The Use of DFT To Predict and Understand Oxidation and Reduction Potentials, Organometallics 32 (2013) 5491–5503.

[58] I. Hoskovcová, J. Roháčová, D. Dvořák, T. Tobrman, S. Záliš, R. Zvěřinová, J. Ludvík, Synthesis and electrochemical study of iron, chromium and tungsten aminocarbenes: Role of ligand structure and central metal nature, Electrochim. Acta 55 (2010) 8341–8351.

[59] M. Landman, R. Pretorius, R. Fraser, B.E. Buitendach, M.M. Conradie, P.H. van Rooyen, J. Conradie, Electrochemical behaviour and structure of novel phosphine- and phosphite-substituted tungsten(0) Fischer carbene complexes, Electrochim. Acta 130 (2014) 104–118.

[60] C. Baldoli, P. Cerea, L. Falciola, C. Giannini, E. Licandro, S. Maiorana, P. Mussini, D. Perdicchia, The electrochemical activity of heteroatom-stabilized Fischer-type carbene complexes, J. Organomet. Chem. 690 (2005) 5777–5787.

[61] N. Camire, A. Nafady, W.E. Geiger, Characterization and reactions of previously elusive 17-electron cations: electrochemical oxidations of $(C_6H_6)Cr(CO)_3$ and $(C_5H_5)Co(CO)_2$ in the presence of $[B(C_6F_5)_4]^-$, J. Am. Chem. Soc. 124 (2002) 7260–7261.

[62] N. Camire Ohrenberg, L.M. Paradee, R.J. DeWitte, D. Chong, W.E. Geiger, Spectra and synthetic-time-scale substitution reactions of electrochemically produced $[Cr(CO)_3(\eta^6\text{-Arene})]^+$ complexes, Organometallics 29 (2010) 3179–3186.

[63] N.J. Stone, D.A. Sweigart, A.M. Bond, Effects of temperature and supporting electrolyte on the electrochemical oxidation of (benzene)tricarbonylchromium and other π-hydrocarbon complexes, Organometallics 5 (1986) 2553–2555.

[64] L.K. Yeung, J.E. Kim, Y.K. Chung, P.H. Rieger, D.A. Sweigart, Control of ligand substitution and addition reactions of (arene)$Cr(CO)_3$ complexes by attachment of a self-closing redox switch, Organometallics 15 (1996) 3891–3897.

[65] Y. Li, J.E. McGrady, T. Baer, Metal−benzene and metal−CO bond energies in neutral and ionic $C_6H_6Cr(CO)_3$ Studied by threshold photoelectron−photoion coincidence spectroscopy and density functional theory, J. Am. Chem. Soc. 124 (2002) 4487–4494.

ACCEPTED MANUSCRIPT

SYNOPSIS

Novel isomeric *N*,*N*-dimethylaniline and anisole monocarbene complexes and carbene-heteroarene chelates, π-bonded to $Cr(CO)_3$, are isolated, including a unique heterotrimetallic biscarbene complex with a σ-,σ-,π-coordination mode of the arene ligand. HOMO location and electron transfer processes are investigated through electrochemistry and spectroelectrochemistry techniques and their assignment is supported by DFT calculations and by comparing the oxidation and reduction potentials of the individual metal entities.

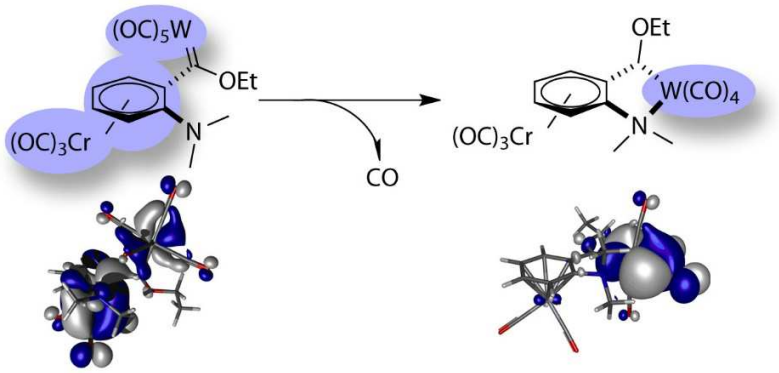

ACCEPTED MANUSCRIPT

ACCEPTED MANUSCRIPT

Highlights

- We report the synthesis of heterobi- and heterotrimetallic W Fischer carbene complexes of a (η^6-RC_6H_5)$Cr(CO)_3$ fragment with the ligand in σ,π- ($\mu,\eta^{6:1}$-) or σ,σ,π- ($\mu_3,\eta^{6:1:1}$-) coordination modes.
- For R = NMe_2, all three different isomers of the heterobimetallic Cr,W complexes have been prepared under the conditions of either kinetic or thermodynamic control
- Thermal or photochemical substitution of one CO ligand at the carbene site grant access to {$W(CO)_4$} carbene complexes with a chelate bonding of the heteroatom substituent
- Electrochemical and IR-spectroelectrochemical studies confirm the primary oxidation site changes from the (η^6-arene)$Cr(CO)_3$ fragment in the $W(CO)_5$ carbene complexes to the carbene fragment in the $W(CO)_4$ chelate complexes
- The experimentally derived order of redox events was confirmed by backing quantum chemical calculations

ACCEPTED MANUSCRIPT